American Mineralogist, Volume 77, pages 685–703, 1992

Crystalline solution series and order-disorder within the natrolite mineral group*

Malcolm Ross, Marta J. K. Flohr
U.S. Geological Survey, MS 959, Reston, Virginia 22092, U.S.A.
Daphne R. Ross
Smithsonian Institution, Department of Mineral Sciences, Washington, DC 20560, U.S.A.

Abstract

The zeolite minerals of the natrolite group (natrolite, tetranatrolite, paranatrolite, mesolite, scolecite, thomsonite, gonnardite, edingtonite, and tetraedingtonite) have the general formula $(Na,Ca,Ba)_{8-16}(Al,Si)_{40}O_{80}\cdot nH_2O$. Electron microprobe and X-ray analyses were made of natrolite, tetranatrolite, gonnardite, and thomsonite from the Magnet Cove alkaline igneous complex, Arkansas, and of selected specimens from the U.S. National Museum. This information and data from the literature indicate that natrolite, mesolite, scolecite, edingtonite, and tetraedingtonite show only small deviations from the ideal stoichiometry. In contrast, gonnardite, tetranatrolite, and thomsonite show large deviations from the ideal end-member compositions and compose three crystalline series. These are (1) the gonnardite series given by $\square_x Na_{16-3x}Ca_{2x}Al_{16+x}Si_{24-x}O_{80}\cdot nH_2O$, where x varies from approximately 0.3 to 3.2 and $\square$ denotes a cation vacancy in the intraframework channels, (2) the tetranatrolite series given by $\square_0 Na_{16-x}Ca_xAl_{16+x}Si_{24-x}O_{80}\cdot 16H_2O$, where x varies from approximately 0.4 to 4, and (3) the thomsonite series given by $\square_4 Na_{4+x}Ca_{8-x}Al_{20-x}Si_{20+x}O_{80}\cdot 24H_2O$, where x varies from approximately 0 to 2. The structures of the natrolite minerals are composed of chains of AlO_4 and SiO_4 tetrahedra that link in one of three ways to form the natrolite-, thomsonite-, or edingtonite-type frameworks. The intraframework channels are occupied by $NaO_4(H_2O)_2$, $(Na,Ca)O_4(H_2O)_2$, $CaO_4(H_2O)_3$, $CaO_4(H_2O)_2$, $(Na,Ca)O_4(H_2O)_4$, or $BaO_6(H_2O)_4$ polyhedra. The Na-bearing polyhedra are edge linked to form continuous chains, whereas the Ca and Ba polyhedra are isolated from one another by channel vacancies. The structures of the natrolite minerals are defined by combining each of the three types of framework structures with various combinations of channel-occupying polyhedra. Various polysomatic series can be constructed by combining slices of two basic structures to form new hybrid structures. The compositional variation and complex crystallography of gonnardite can be explained if the gonnardite series is a polysomatic series composed of mixed domains of natrolite and thomsonite. A paranatrolite series ($\square_0 Na_{16-x}Ca_xAl_{16+x}Si_{24-x}O_{80}\cdot 24H_2O$) is predicted, and it is proposed that the structure of paranatrolite combines the natrolite framework with channel-filling $NaO_4(H_2O)_2$ and $(Na,Ca)O_4(H_2O)_4$ polyhedra.

Introduction

The minerals of the natrolite group are commonly found as later-stage crystallization products within cavities in basaltic rocks, in various hydrothermal deposits, and as alteration products of nepheline in nepheline syenites, phonolites, and related rocks. The latter type of occurrence was noted in our studies of various syenites from the Magnet Cove alkaline igneous complex located near Hot Springs, Arkansas (Flohr and Ross, 1989, 1990). Since many of the minerals in these rocks are extensively metasomatized, one of the purposes of our Magnet Cove investigations was to characterize the mineralization and recrystallization processes occurring during emplacement and cooling of the igneous rocks and to relate these processes to mineralization of the adjacent country rocks. Some of the replacement or overgrowth textures noted in the more mafic syenites are sodic pyroxenes and amphiboles replacing diopside, augite, and hedenbergite; F- and OH-rich grandite series garnets overgrowing schorlomite and melanite; phlogopite and biotite replacing clinopyroxene; and titanite appearing as overgrowths on perovskite. Nepheline is replaced by one or more of the following minerals during middle-stage magmatic crystallization: feldspar, cancrinite, sodalite, and nosean. During late-stage crystallization, natrolite, thomsonite, gonnardite, and tetranatrolite may replace nepheline.

The present paper gives new data on the crystallography and composition of four members of the natrolite

* Adapted from the Presidential Address of Malcolm Ross, given at the annual meeting of the Mineralogical Society of America on October 22, 1991, in San Diego, California.

0003–004X/92/0708–0685$02.00

mineral group found in the Magnet Cove rocks. To verify the Magnet Cove studies, a reexamination was made of selected specimens from the U.S. National Museum representing six of the nine members of this mineral group. The new chemical and crystallographic data obtained on the museum specimens are integrated with that obtained from the Magnet Cove samples to give new insights into the nature of the crystalline solution series within the natrolite mineral group.

Analytical methods

Light optical and electron microprobe analyses of the zeolites replacing nepheline were made on polished thin sections of various alkaline rocks from the Magnet Cove igneous intrusion and on polished thin sections of single crystals of selected natrolite group minerals obtained from the U.S. National Museum (USNM). Mineral compositions were obtained using an automated ARL-SEMQ[1] electron microprobe. The method of chemical analysis is given by Flohr and Ross (1989, p. 114), with the following modifications. To minimize Na loss, we generally used a defocused, unrastered electron beam 30 μm in diameter operating at 15 kV and with a 0.1-μA beam current. Analysis times were generally for 20 s. The accuracy of the analyses was verified by reanalysis of feldspar standards, by comparison with analyses made by rastering over a large volume of the crystal, and by using longer and shorter analysis times. Our analyses showed that Na loss could not be detected during the 20-s analyses when the beam diameter was greater than 15–20 μm. Analysis for H_2O content in these minerals was not made; thus the oxides sums are 12–17% low, depending on the amount of H_2O in the crystal structure. When the wt% H_2O expected for natrolite, tetranatrolite, mesolite, scolecite, or thomsonite is added to the oxide sums, totals tend to be less than 100%. Except for H_2O, we do not believe that any significant amounts of other chemical components remained undetected. We note that other reported electron probe analyses of the natrolite group minerals also show low sums (e.g., Kile and Modreski, 1988, Table 6; Birch, 1989, Table 9; Nawaz, 1988, Tables 2, 3).

Some of our samples were examined with the JEOL-840 scanning electron microscope. Crystallographic characterization was made of the samples using the optical microscope, the single-crystal Buerger precession X-ray camera, and the automated Scintag powder X-ray diffractometer. The crystal drawings presented in this paper were made using computer software written by Dowty (1991).

Chemical compositions of the natrolite group minerals

End-member and generalized chemical formulas of the nine known members of the natrolite mineral group are listed in Table 1. All formulas are normalized to Si + Al = 40 (80 O atoms) so as to facilitate comparison of the mineral species. The numbers of formula units (Z) per unit cell are based on the crystallographic data given in Table 2. For a comprehensive discussion of the previous studies of these minerals, the reader is referred to Gottardi and Galli (1985).

Table 1. Names, chemical formulas, and unit-cell content of the members of the natrolite mineral group

Mineral name	Chemical formula	Z*
Natrolite	$Na_{16}Al_{16}Si_{24}O_{80}\cdot 16H_2O$	1
Tetranatrolite	$(Na,Ca)_{16}(Al,Si)_{40}O_{80}\cdot 16H_2O$	½
Paranatrolite	$(Na,Ca)_{16}(Al,Si)_{40}O_{80}\cdot 24H_2O$**	1
Scolecite	$Ca_8Al_{16}Si_{24}O_{80}\cdot 24H_2O$	1
Mesolite	$Na_{5.33}Ca_{5.33}Al_{16}Si_{24}O_{80}\cdot 21.33H_2O$	3
Thomsonite	$(Na,Ca)_{12}(Al,Si)_{40}O_{80}\cdot 24H_2O$	1
Gonnardite	$(Na,Ca)_{12-15}(Al,Si)_{40}O_{80}\cdot nH_2O$	?
Edingtonite	$Ba_8Al_{16}Si_{24}O_{80}\cdot 32H_2O$	¼
Tetraedingtonite	$Ba_8Al_{16}Si_{24}O_{80}\cdot 32H_2O$	¼

* Z value based on unit-cell data given in Table 2.
** H_2O content was calculated (Chao, 1980).

Natrolite minerals from the Magnet Cove alkaline igneous complex

In examining the various syenites from the Magnet Cove igneous complex, the following minerals, in addition to feldspar, were observed to replace nepheline: (1) natrolite and cancrinite in ijolite 1-166B, (2) tetranatrolite and nosean in jacupirangite 86-53A, (3) analcite, gonnardite, and thomsonite in jacupirangite H-45-8 (Fig. 1A), and (4) gonnardite and thomsonite in ijolite 85-16A (Fig. 1B). In nepheline syenite 2-DJ7, natrolite and sodalite replace feldspar. The compositional trends of coexisting gonnardite and thomsonite in ijolite 85-16A and in jacupirangite H-45-8 are plotted in Figures 2 and 3, respectively. Also plotted in Figure 2 are six analyses of natrolite (USNM 126671). These figures show the very large chemical variation in the gonnardite series, ranging in composition from that very close to end-member natrolite ($Na_{16}Al_{16}Si_{24}O_{80}\cdot 16H_2O$) to a composition approaching that of end-member thomsonite ($Na_4Ca_8Al_{20}Si_{20}O_{80}\cdot 24H_2O$). Relative to gonnardite, the thomsonite in these rocks shows a more restricted composition range. Selected analyses of gonnardite and thomsonite that are plotted in Figure 2 are compiled in Tables 3 and 4. Analyses of tetranatrolite from jacupirangite 86-53A are given in Table 5.

The compositional trends for gonnardite, thomsonite, and tetranatrolite, so clearly delineated in the Magnet Cove rocks, have not been adequately described in the literature (see Foster, 1965a; Nawaz, 1988). Because of the poor understanding of the compositional ranges of several of the natrolite minerals, we decided to examine a number of well-crystallized USNM samples of six of the nine known natrolite minerals to see if compositional trends noted in the Magnet Cove samples could be found in samples from other localities.

[1] Any use of trade names in this report is for descriptive purposes only and does not imply endorsement by the U.S. Geological Survey.

TABLE 2. Crystallographic and locality data for the natrolite minerals

Mineral name	Space group	a (Å)	b (Å)	c (Å)	z*	Locality (sample no.)**	Reference
Natrolite (orthorhombic)	*Fdd2*	18.31	18.67	6.60	1	Mont Saint-Hilaire, Quebec (USNM R18930)	present study
	Fdd2	18.29	18.64	6.56	1	Bound Brook, New Jersey (USNM 126671)	present study
	Fdd2	18.31	18.60	6.59	1	clear crystals, Puy de Dome, France (USNM R16517)	present study
	Fdd2	18.32	18.62	6.59	1	cloudy cracked crystals, Puy de Dome, France (USNM R16517)	present study
	Fdd2	18.272	18.613	6.593	1	Dutoitspan, South Africa (CU 193466)	Artioli et al. (1984)
Tetranatrolite (tetragonal)	*I42d*	13.141		6.617	½	Mont Saint-Hilaire, Quebec (USNM R18930)	present study
	I42d	13.08		6.624	½	Kloech, Austria† (USNM 158913)	present study
	I42d	13.074		6.620	½	Marianberg, Bohemia	Pechar (1989)
	I42d	13.21		6.622	½	Tvedalen, Norway	Mazzi et al. (1986)‡
Paranatrolite (orthorhombic)	F***	19.07	19.13	6.580	1	Mont Saint-Hilaire, Quebec	Chao (1980)
Scolecite (monoclinic)	*Fd*	18.49	18.98 (β = 90.72°)	6.523	1	India (USNM 149846)	present study
	Fd	18.508	18.981 (β = 90.64°)	6.527	1	Berufjord, Iceland	Joswig et al. (1984)
Mesolite (orthorhombic)	*Fdd2*	18.44	56.85	6.58	3	Poona, India (USNM 155046)	present study
	Fdd2	18.4049	56.655	6.5443	3	Poona, India	Artioli et al. (1986)
Thomsonite (orthorhombic)	*Pncn*	13.15	13.06	13.26	1	Honshu, Japan (USNM 147446)	present study
	Pmc2$_1$ or *P2cm* or *Pmcm*	13.08	13.04	13.20	1	Drain, Oregon (USNM 140406)	present study
	Pncn?	13.08	13.09	13.22	1	Table Mt., Colorado (USNM C3615)	present study
	Pncn	13.1043	13.0569	13.2463	1	unknown (CU 2882)	Ståhl et al. (1990)
Gonnardite (orthorhombic?)		18.56	18.64 (pseudocell)	6.62	1	Styria, Austria (USNM R10022)	present study
Eddingtonite (orthorhombic)	*P2,2,2*	9.550	9.665	6.523	¼	Westergotland, Sweden (no. 1505)	Galli (1976)
Tetraldingtonite (tetragonal)	*P42,m*	9.584		6.524	¼	Kilpatrick Hills, Scotland	Mazzi et al. (1984)

* Value of *z* based on chemical formula units given in Table 1.

** Other samples studied: from Puy de Dome, France—gonnardite-thomsonite (157727), gonnardite-thomsonite (15273), gonnardite (138378); from Maluti Mts., Lesotho—scolecite (143136).

† Crystal of tetranatrolite found in gonnardite sample 158913 from Kloech, Austria.

‡ Crystal structure was reported to be of "gonnardite"; the structure is actually of tetranatrolite (see text).

Natrolite minerals from the U.S. National Museum collections

The museum samples, including three natrolite, two tetranatrolite, two scolecite, one mesolite, six thomsonite, and five gonnardite samples, were examined; their localities and unit-cell and space group data, plus information on other studies in the literature, are given in Table 2. One of the samples (R18930) contains coexisting natrolite and tetranatrolite, one (158913) contains coexisting tetranatrolite and gonnardite, one contains two types of natrolites (R16517), and three (R10022, 157727, 15273) contain coexisting gonnardite and thomsonite.

Natrolite. The compositions of natrolite samples 126671 and R18930 are plotted in Figures 2, 4, and 5; the average compositions of natrolite samples 126671, R18930, and R16517 are given in Table 6. Natrolite shows very little compositional variation. Of the 44 analyses summarized in Table 6, CaO, MgO, Fe_2O_3, and BaO were not detected, and only small amounts of SrO (0.05%) and K_2O (0.02%) were observed. It appears from our work that the intraframework channels in natrolite contain essentially Na and H_2O molecules with only very small amounts, if any, of Sr and K replacing Na. Ca does not appear to enter the natrolite structure. There is some indication that the Na content is somewhat less than the ideal 16 atoms per formula unit; Na averages 15.42 atoms for the 44 natrolite analyses summarized in Table 6. This apparent deficiency of Na could be attributed to Na loss during electron probe analysis, however, the older wet chemical analyses also show such a deficiency; for example, see Nawaz (1988), Foster (1965b), and Deer et al. (1963).

Tetranatrolite and paranatrolite. Selected chemical analyses of Mont Saint-Hilaire tetranatrolite R18930 and Magnet Cove tetranatrolite 86-53A are presented in Table 5; their compositions are plotted in Figure 5 and lie

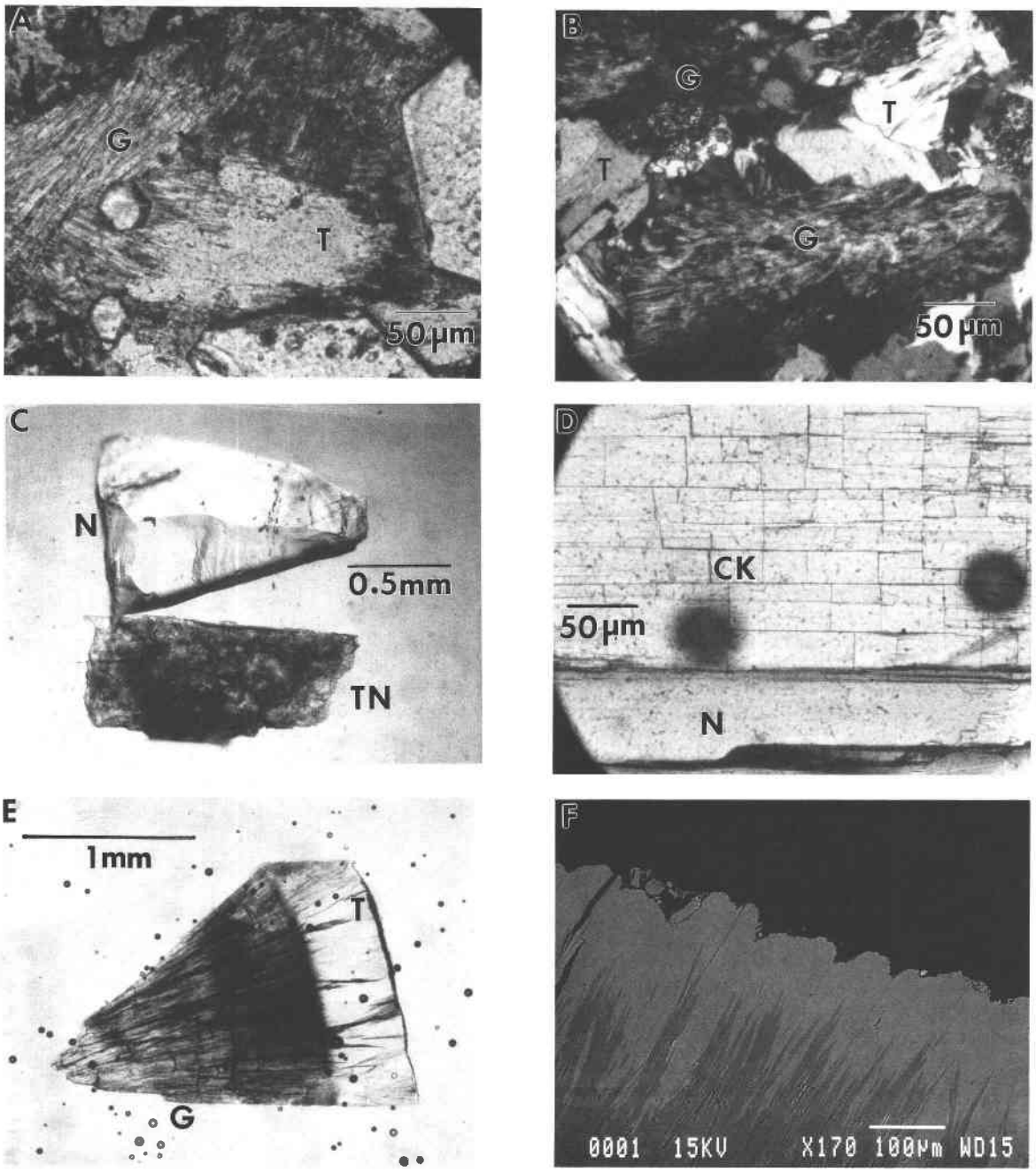

Fig. 1. (**A**) Photomicrograph (plain light) of a polished section of Magnet Cove jacupirangite H-45-8 showing fibrous gonnardite (G) and platy thomsonite (T). (**B**) Polished section photomicrograph (polarized light) of Magnet Cove ijolite 85-16A showing fibrous gonnardite (G) and platy thomsonite (T). (**C**) Grain-mount polished section photomicrograph (plain light) of a natrolite crystal (N) and a tetranatrolite crystal (TN) from sample R18930 from Mont Saint-Hilaire, Quebec. (**D**) Grain-mount polished section photomicrograph (plain light) of a composite crystal from sample R16517 from Puy de Dome, France. The clear area is composed of natrolite (N), and the area with numerous cracks (CK) is composed of twinned natrolite and a second phase, both of which probably formed by decomposition of paranatrolite. (**E**) Grain-mount polished section photomicrograph (plain light) of a segment of a spherule from sample 157727 from Puy de Dome, France. The dark core area is composed of acicular gonnardite (G); the light rim area is composed of thomsonite (T). (**F**) Backscattered electron (BSE) image from a grain-mount polished section of sample R10022 from Styria, Austria. The acicular gonnardite (darker areas) interfingers with thomsonite (lighter areas) that composes the rim of the spherule. Electron microprobe analyses were made of all the natrolite minerals in these polished sections.

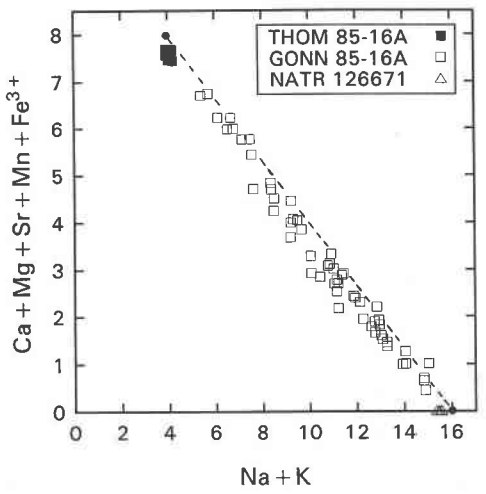

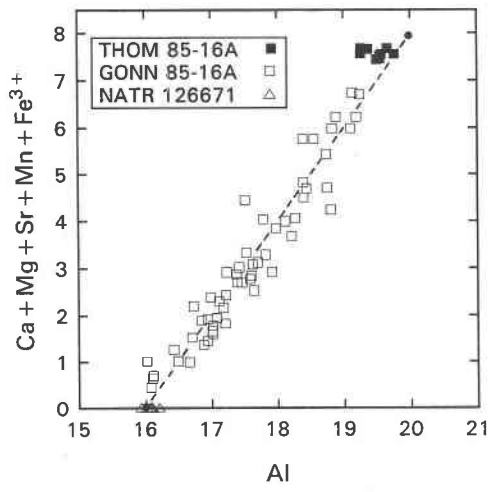

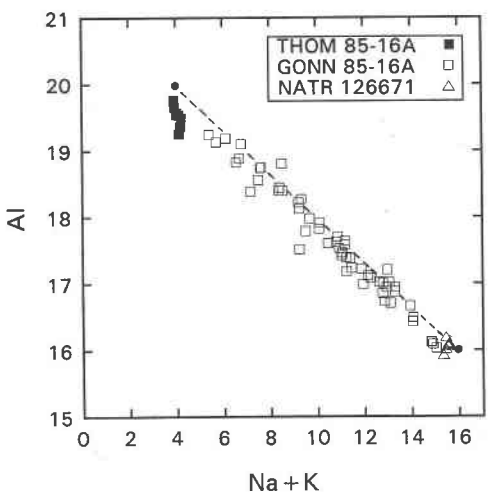

Fig. 2. Compositional trends in terms of atoms per formula unit (Table 1) of coexisting gonnardite and thomsonite in ijolite 85-16A from the Magnet Cove igneous complex, Arkansas. Also plotted are compositions of natrolite 126671. Small closed circles show the compositions of end-member natrolite ($Na_{16}Al_{16}Si_{24}O_{80}\cdot 16H_2O$) and end-member thomsonite ($Na_4Ca_8Al_{20}Si_{20}O_{80}\cdot 24H_2O$).

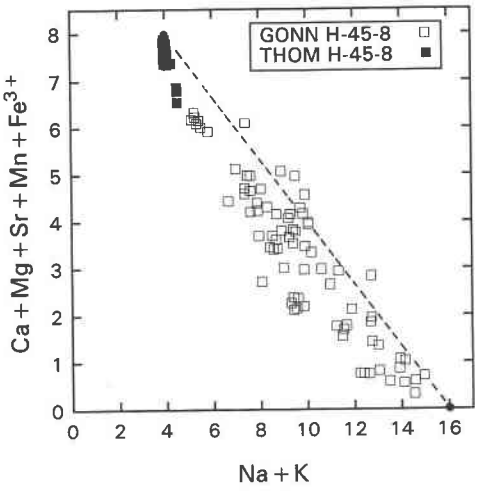

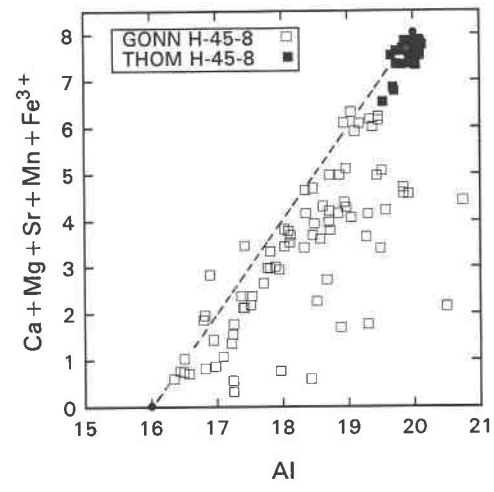

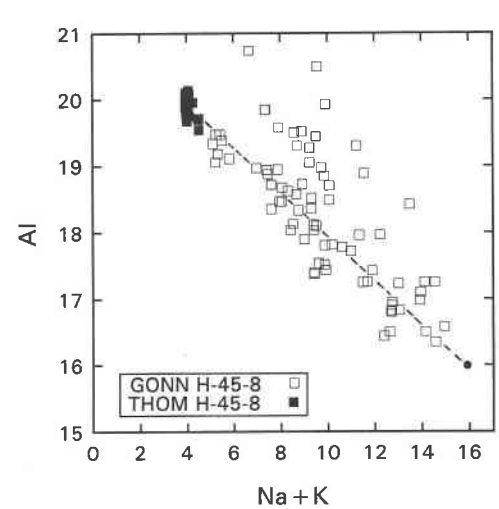

Fig. 3. Compositional trends of coexisting gonnardite and thomsonite in jacupirangite H-45-8 from the Magnet Cove igneous complex. Small closed circles as in Figure 2.

TABLE 3. Selected electron microprobe analyses of three gonnardite samples

	Gonnardite											
USNM no.	R10022 23	R10022 27	R10022 35	158913 3	158913 78	158913 79	85-16A 38	85-16A 39	85-16A 44	85-16A 45	85-16A 46	85-16A 51
						Wt%						
SiO_2	40.93	40.44	42.57	42.20	43.94	45.29	40.63	42.33	44.68	45.47	39.18	43.69
Al_2O_3	29.13	29.69	27.93	27.46	27.40	27.14	26.84	28.00	26.42	25.80	28.28	26.64
Fe_2O_3*	0.04	nd	nd	nd	nd	nd	0.02	0.13	0.11	0.47	0.08	0.19
MgO	0.05	0.08	0.05	0.06	0.05	0.02	nd	0.22	0.19	0.00	0.04	0.17
CaO	6.94	6.11	4.86	5.09	2.71	0.82	7.48	5.44	1.89	1.46	9.63	3.48
BaO	0.02	nd	0.05	nd	nd	nd	0.08	nd	0.02	0.07	0.05	0.04
SrO	0.33	0.29	0.07	0.10	0.08	0.04	na	na	na	na	na	na
Na_2O	8.98	10.23	11.25	9.98	12.97	14.93	8.60	10.60	13.73	14.69	6.69	12.44
K_2O	0.03	0.02	nd	0.03	0.02	nd	0.03	0.04	0.02	0.04	0.02	0.02
Sum**	86.45	86.86	86.78	84.92	87.17	88.24	83.68	86.76	87.06	88.00	83.97	86.67
						Cations based on formula unit with Si + Al = 40						
Si	21.753	21.445	22.557	22.639	23.056	23.443	22.490	22.477	23.572	23.970	21.614	23.274
Al	18.247	18.555	17.443	17.361	16.944	16.557	17.510	7.523	16.428	16.030	18.386	16.726
	40	40	40	40	40	40	40	40	40	40	40	40
Fe^{3+}	0.018	—	—	—	—	—	0.009	0.053	0.044	0.185	0.032	0.076
Mg	0.040	0.063	0.039	0.045	0.039	0.015	—	0.174	0.149	0.000	0.033	0.135
Ca	3.952	3.471	2.759	2.926	1.524	0.455	4.436	3.095	1.068	0.825	5.692	1.986
Ba	0.004	nd	0.010	—	—	—	0.017	0.000	0.004	0.014	0.011	0.008
Sr	0.102	0.089	0.022	0.031	0.024	0.012	—	—	—	—	—	—
	4.115	3.624	2.830	3.002	1.587	0.482	4.462	3.322	1.265	1.024	5.768	2.205
Na	9.254	10.518	11.558	10.383	13.195	14.984	9.230	10.913	14.044	15.015	7.155	12.849
K	0.020	0.014	—	0.020	0.013	0.000	0.021	0.027	0.013	0.027	0.014	0.014
	9.274	10.532	11.558	10.403	13.208	14.984	9.251	10.940	14.057	15.042	7.169	12.863
Cation sum	53.389	54.156	54.388	53.403	54.795	55.466	53.713	54.262	55.322	56.066	52.937	55.068

Note: nd = not detected, na = not analyzed.
* Total Fe reported as Fe^{3+}.
** H_2O content of gonnardite is unknown.

TABLE 4. Selected electron microprobe analyses of five thomsonite samples

	Thomsonite											
No.	R10022 8	R10022 9	R10022 37	147446 22	147446 70	140406 86	140406 90	C3615 13	C3615 63	C3615 66	85-16A 32	85-16A 35
						Wt%						
SiO_2	38.64	38.57	38.32	36.33	35.10	40.15	39.06	40.78	40.39	39.67	36.81	37.04
Al_2O_3	29.14	29.47	30.21	29.05	30.16	28.96	30.17	28.14	29.45	30.16	30.51	29.18
Fe_2O_3*	nd	nd	0.06	0.03	0.02	0.03	nd	nd	0.02	0.02	0.07	0.06
MgO	0.14	0.14	0.15	0.02	0.14	0.15	0.15	nd	0.13	0.16	0.04	0.02
CaO	11.71	10.70	11.13	9.75	8.93	11.57	11.57	10.47	10.50	11.23	12.73	12.55
BaO	0.02	0.08	nd	nd	nd	nd	nd	nd	nd	0.06	0.16	0.03
SrO	1.35	1.59	1.88	6.53	6.76	0.62	0.83	0.20	0.23	0.27	na	na
Na_2O	4.13	4.81	4.69	3.88	3.69	4.61	4.83	5.35	5.38	4.75	3.69	3.84
K_2O	0.08	0.06	0.07	nd	0.02	nd	nd	nd	nd	nd	nd	nd
Sum	85.21	85.42	86.51	85.59	84.82	86.09	86.61	84.94	86.10	86.32	84.01	82.72
H_2O**	13.40	13.40	13.40	13.40	13.40	13.40	13.40	13.40	13.40	13.40	13.40	13.40
Sum	98.61	98.82	99.91	98.99	98.22	99.49	100.01	98.34	99.50	99.72	97.41	96.12
						Cations based on formula unit with Si + Al = 40						
Si	21.177	21.047	20.735	20.593	19.874	21.621	20.939	22.060	21.513	21.097	20.234	20.742
Al	18.823	18.953	19.265	19.407	20.126	18.379	19.061	17.940	18.487	18.903	19.766	19.258
	40	40	40	40	40	40	40	40	40	40	40	40
Fe^{3+}	—	—	0.023	0.014	0.009	0.014	—	—	0.009	0.009	0.028	0.023
Mg	0.114	0.114	0.121	0.017	0.118	0.120	0.120	—	0.103	0.127	0.033	0.017
Ca	6.876	6.256	6.452	5.921	5.417	6.675	6.645	6.068	5.992	6.399	7.497	7.530
Ba	0.004	0.017	—	—	—	—	—	—	—	0.013	0.034	0.007
Sr	0.429	0.503	0.590	2.146	2.219	0.194	0.258	0.063	0.071	0.083	—	—
	7.423	6.890	7.186	8.098	7.763	7.003	7.023	6.131	6.175	6.631	7.592	7.577
Na	4.389	5.089	4.920	4.264	4.051	4.813	5.020	5.611	5.556	4.898	3.933	4.169
K	0.056	0.042	0.048	—	0.014	—	—	—	—	—	—	—
	4.445	5.131	4.968	4.264	4.065	4.813	5.020	5.611	5.556	4.898	3.933	4.169
Cation sum	51.868	52.021	52.154	52.362	51.828	51.816	52.043	51.742	51.731	51.529	51.525	51.746

Note: nd = not detected, na = not analyzed.
* Total Fe reported as Fe^{3+}.
** Weight percent H_2O calculated on the basis of $24H_2O$ per formula unit (Table 1).

TABLE 5. Selected electron microprobe analyses of cloudy crystals from sample R16517 and tetranatrolite R18930 and 86-53A

Mineral USNM no.	Nat* R16517 (14)**	Tetra R18930 77	Tetra R18930 74	Tetra 86-53A 12	Tetra 86-53A 18	Tetra 86-53A 23
			Wt%			
SiO_2	45.19	38.21	39.07	39.17	40.59	37.85
Al_2O_3	26.50	29.61	28.55	30.34	29.32	31.26
Fe_2O_3†	nd	nd	0.04	0.04	0.12	0.11
MgO	nd	nd	nd	0.04	0.04	0.10
CaO	0.35	5.00	3.61	5.26	4.11	6.68
BaO	nd	nd	nd	nd	0.05	nd
SrO	0.04	0.34	1.06	nd	nd	nd
Na_2O	15.42	11.78	12.18	11.94	12.67	11.41
K_2O	0.02	0.02	0.02	0.02	0.07	nd
Sum	87.52	84.96	84.53	86.81	86.97	87.40
H_2O‡	9.48	9.48	9.48	9.48	9.48	9.48
Sum	97.00	95.44	94.01	96.29	96.45	96.88
	Cations based on formula unit with Si + Al = 40					
Si	23.651	20.906	21.491	20.911	21.606	20.270
Al	16.349	19.094	18.509	19.089	18.394	19.730
	40	40	40	40	40	40
Fe^{3+}	—	—	0.018	0.018	0.049	0.045
Mg	—	—	—	0.032	0.032	0.080
Ca	0.194	2.931	2.128	3.009	2.344	3.833
Ba	—	—	—	—	0.010	—
Sr	0.012	0.108	0.338	—	—	—
	0.206	3.039	2.484	3.059	2.435	3.958
Na	15.651	12.496	12.990	12.359	13.076	11.847
K	0.011	0.014	0.014	0.014	0.048	—
	15.662	12.510	13.004	12.373	13.124	11.847
Cation sum	55.868	55.549	55.488	55.432	55.559	55.805

Note: nd = not detected.

* Cloudy cracked crystals are composed of twinned natrolite and a second phase. Sample also contains clear uncracked crystal of untwinned natrolite (Table 6).

** Average of 14 analyses.

† Total Fe reported as Fe^{3+}.

‡ Weight percent H_2O calculated on the basis of $16H_2O$ per formula unit (Table 1).

close to trend line II. The natrolite and tetranatrolite portions of the crystals in our Mont Saint-Hilaire sample are morphologically distinctive—the natrolite portions are clear and colorless without inclusions, whereas the areas of tetranatrolite overgrowth are cloudy white and contain numerous dark inclusions (Fig. 1C). The clear and cloudy phases are easily separated from one another and were identified, using single crystal and powder XRD methods (Table 2), as natrolite and tetranatrolite, respectively. Chen and Chao (1980) have previously reported on the occurrence of thick overgrowths of tetranatrolite on natrolite in specimens from Mont Saint-Hilaire, Quebec, the same locality from which sample R18930 was obtained. The composition of the tetranatrolite in their Mont Saint-Hilaire sample is $(Na,K)_{14.83}Ca_{0.83}(Fe,Ti)_{0.07}Al_{15.66}Si_{24.34}O_{80.51}\cdot 16.58H_2O$. Although the tetranatrolite described by Chen and Chao contains much less Ca than our specimen, its composition plots on the same trend line as ours (Fig. 5, trend II).

Sample R16517, from Puy de Dome, France, is mostly composed of large, clear, colorless crystals of natrolite as shown by single-crystal and powder XRD. However, overgrowths of a second phase appear on the prism faces

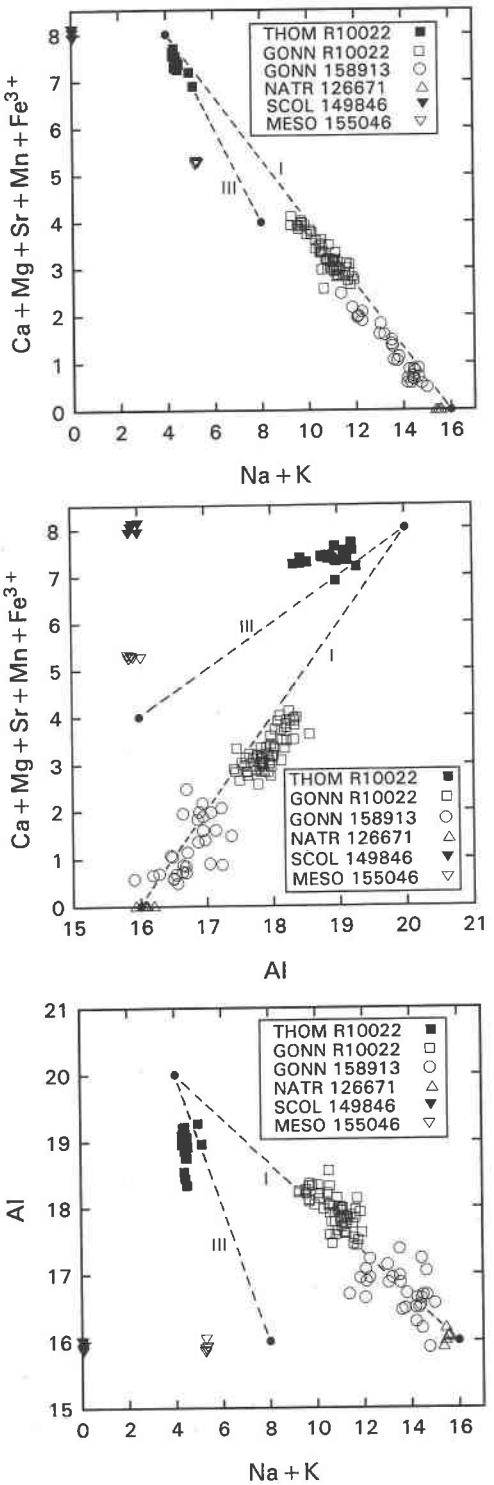

Fig. 4. Compositional trends for USNM samples of thomsonite, gonnardite, natrolite, scolecite, and mesolite. Small closed circles show the compositions of end-member natrolite, scolecite, and mesolite (Table 1) and end-member thomsonite on the join $Na_4Ca_8Al_{20}Si_{20}O_{80}$-$Na_8Ca_4Al_{16}Si_{24}O_{80}$. Dashed lines I and III show the gonnardite and thomsonite series trends, respectively. Small closed circles at the ends of trend III define the ideal end-member thomsonite, $Na_4Ca_8Al_{20}Si_{20}O_{80}\cdot 24H_2O$, and a hypothetical end-member, $Na_8Ca_4Al_{16}Si_{24}O_{80}\cdot 24H_2O$.

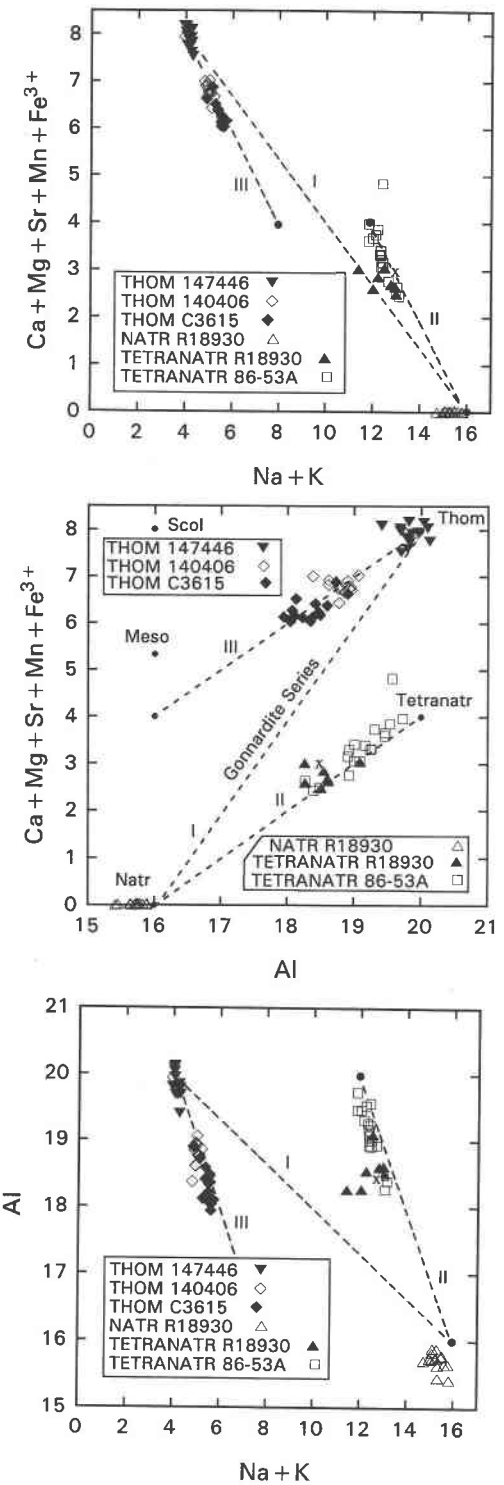

Fig. 5. Compositional trends for thomsonite, natrolite, and tetranatrolite from the USNM samples and for tetranatrolite from Magnet Cove jacupirangite 86-53A. Dashed line II shows the tetranatrolite series trend, and the small closed circle at the high Ca end of this trend defines the theoretical tetranatrolite end-member, $Na_{12}Ca_4Al_{20}Si_{20}O_{80} \cdot 16H_2O$. Trends I and III and the other closed circles are defined in Figure 4. The "x" gives the composition of tetranatrolite from Norway (Mazzi et al., 1986).

TABLE 6. Averages of electron microprobe analyses of U.S. National Museum samples of natrolite, mesolite, and scolecite

Mineral	Nat	Nat**	Nat	Meso	Scol	Scol
USNM no.	126671	R16517	R18930	155046	143136	149846
*N**	(7)	(16)	(21)	(5)	(7)	(5)
			Wt%			
SiO_2	46.12	45.80	46.37	45.31	45.14	44.50
Al_2O_3	26.25	26.28	25.44	25.36	25.33	24.99
Fe_2O_3†	nd	nd	nd	nd	0.06	nd
MgO	nd	nd	nd	nd	nd	nd
CaO	nd	nd	nd	9.18	13.74	13.77
BaO	nd	nd	nd	nd	nd	nd
SrO	0.05	0.05	0.06	0.07	0.07	0.06
Na_2O	15.41	15.46	14.99	5.08	0.11	0.04
K_2O	0.02	0.02	0.02	0.02	nd	nd
Sum	87.85	87.62	86.88	85.02	84.45	83.36
H_2O‡	9.48	9.48	9.48	12.37	13.78	13.78
Sum	97.33	97.10	96.36	97.39	98.23	97.14
	Cations based on formula unit with Si + Al = 40					
Si	23.941	23.862	24.293	24.102	24.078	24.069
Al	16.059	16.138	15.707	15.898	15.922	15.931
	40	40	40	40	40	40
Fe^{3+}	—	—	—	—	0.024	—
Mg	—	—	—	—	—	—
Ca	—	—	—	5.232	7.853	7.978
Ba	—	—	—	—	—	—
Sr	0.015	0.014	0.017	0.020	0.023	0.018
	0.015	0.014	0.017	5.252	7.900	7.996
Na	15.509	15.620	15.232	5.239	0.114	0.040
K	0.013	0.012	0.014	0.011	—	—
	15.522	15.632	15.246	5.250	0.114	0.040
Cation sum	55.537	55.646	55.263	50.502	48.014	48.036

Note: nd = not detected.
* *N* = number of analyses in the average.
** Analyses of clear uncracked natrolite crystals. Sample also contains cloudy cracked crystals composed mostly of twinned natrolite (Table 5).
† Total Fe reported as Fe^{3+}.
‡ Weight percent H_2O calculated on the basis of formulas given in Table 1.

of some of the natrolite crystals—a morphology very similar to the overgrowths of tetranatrolite on natrolite found in the Mont Saint-Hilaire sample (Chen and Chao, 1980, Figs. 1, 2). The overgrowth areas in sample R16517 have a distinctive appearance in that they are cloudy white in color and contain numerous cracks and inclusions. These defects are absent in the clear natrolite cores. Clear and cracked areas in a grain-mount polished section are shown in Figure 1D. Oil immersion mounts of crystal fragments that are riddled with cracks have anomalous optical properties and show a laminar texture under crossed polarizers. Some of the cloudy grains have large fractures that are oriented perpendicular to the **c** axis. The nearly identical X-ray powder patterns of the clear and cloudy crystals show them to be natrolite, with the exception that a very weak extra peak occurs at 6.81 Å in the pattern of the latter. The single-crystal X-ray patterns of the cloudy crystals give unit-cell dimensions very close to those of the clear natrolite (Table 2). The cloudy crystals are twinned by a **c** axis rotation of 90°, as shown by the exact coincidence of the **a*** and **b*** axes in the precession photographs (see Pabst, 1971; Chen and Chao, 1980). There is no X-ray evidence for the presence of tetranatrolite in this sample, but the 6.81-Å peak seen in the X-ray pow-

der pattern may be the 220 reflection of residual paranatrolite. The chemical compositions of the clear and cracked areas, although very similar, are distinctive. Fourteen analyses (averaged in Table 5) of the areas with cracks showed CaO to be present, ranging from 0.12 to 0.48 wt%. Of the 16 analyses (averaged in Table 6) of the clear uncracked areas, 13 showed no detectable CaO and three showed 0.01 wt% CaO.

We propose, in agreement with the observations of Chen and Chao (1980), that the tetranatrolite overgrowths in sample R18930 and the overgrowth areas in sample R16517 are dehydration products of previously formed paranatrolite, a mineral of the natrolite group first described by Chao (1980) as having the composition $Na_{14.00}Ca_{0.80}K_{0.72}Fe_{0.08}Al_{15.60}Si_{24.16}O_{80}\cdot 24H_2O$ and a pseudo-orthorhombic symmetry with $a = 19.07$, $b = 19.13$, and $c = 6.580$ Å.

Mesolite and scolecite. Compositions of mesolite 155046 and scolecite 149846 are plotted in Figure 4, and selected analyses for these specimens as well as for scolecite 143136 are given in Table 6. Crystallographic data are presented in Table 2. Our analyses and those given in the literature (Foster, 1965b; Nawaz et al., 1985; Hey, 1933, 1936; Kile and Modreski, 1988; Alberti et al., 1982) indicate that there is little variation in chemical composition of mesolite and scolecite from the ideal chemical formulas given in Table 1. Rychly and Ulrych (1980) and Ulrych and Rychly (1983) report the overgrowth of mesolite on natrolite and scolecite on mesolite. Gunter et al. (1991) report overgrowths of mesolite on natrolite, both phases having nearly ideal compositions.

Thomsonite and gonnardite. The compositions of thomsonite in single-phase samples 147446, 140406, and C3615 are plotted in Figure 5, and selected analyses are presented in Table 4. X-ray powder and single-crystal analysis (Table 2) confirm the identity of these minerals. The compositions of thomsonite and coexisting gonnardite in sample R10022 and gonnardite sample 158913 are plotted in Figure 4; selected analyses are given in Tables 3 and 4. It is noted that significant amounts of Sr can replace Ca in the thomsonite and tetranatrolite structures (Tables 4, 5).

Thomsonite and gonnardite typically crystallize as spherules or rosettes, which show a distinct radial structure (for example, see Kile and Modreski, 1988, their Figs. 13, 34, 44). The spherules commonly appear within the amygdaloidal cavities of various extrusive igneous rocks. Five samples examined in this study possess a spherulitic habit, and we note that in four of these samples the cores and rims of the spherules are composed of crystals of acicular gonnardite and platy or blocky thomsonite, respectively. The relationship between these two minerals in a segment of a gonnardite-thomsonite spherule from sample 157727 is seen in the light-optical photomicrograph presented in Figure 1E. Details of the gonnardite-thomsonite association at the core-rim interface in a spherule from sample R10022 is seen in the scanning electron micrograph shown in Figure 1F.

Crystalline solution series within the natrolite mineral group

Examination of the chemical composition data given in the tables and figures, coupled with those given in the literature, permits us to define the composition ranges of the Na- and Ca-bearing members of the natrolite mineral group. As discussed above, natrolite, mesolite, and scolecite show a very limited deviation in composition from the ideal formulas given in Table 1 and, thus, do not appear to form any extended crystalline series. An exception to this nearly ideal stoichiometry may occur in natrolite, for in this phase there may be as much as 5% deficiency in Na from the ideal 16 atoms per formula unit (Table 6, natrolite 126671, R16517, R18930; see also Alberti et al., 1982, Table 3). The variability of wet and electron probe chemical analyses, however, makes it difficult to prove unequivocally that such a Na deficiency exists.

In contrast to natrolite, mesolite, and scolecite, the minerals gonnardite, thomsonite, and tetranatrolite show pronounced chemical variation in Na, Ca, Al, and Si content, as delineated in Figures 2, 3, 4, and 5 (trend lines I, II, III). The gonnardite crystalline series lies close the join $Na_{16}Al_{16}Si_{24}O_{80}$-$Na_4Ca_8Al_{20}Si_{20}O_{80}$ (trend line I) and is represented by the formula $\square_x Na_{16-3x}Ca_{2x}Al_{16+x}Si_{24-x}O_{80}\cdot nH_2O$, where $\square$ indicates vacant cation sites within the intraframework channels. Compositional data for gonnardite samples presented in Figures 2, 3, and 4 and in Table 3 show that this series extends from at least $x \cong 0.3$ to $x \cong 3.2$.

The tetranatrolite series lies approximately along the join $Na_{16}Al_{16}Si_{24}O_{80}$-$Na_{12}Ca_4Al_{20}Si_{20}O_{80}$ (trend line II) and is represented by the formula $\square_0 Na_{16-x}Ca_xAl_{16+x}Si_{24-x}O_{80}\cdot 16H_2O$. The data given in Figure 5 and Table 5 show that series II extends from $x \cong 2.4$ to $x \cong 3.9$. The composition given for tetranatrolite by Chen and Chao (1980) and Krogh Anderson et al. (1969), $x = 0.83$ and 0.37, respectively, indicates that series II extends to at least $x \cong 0.4$.

The third series found within the natrolite group is the thomsonite crystalline series. Thomsonite compositions (Table 4; Figs. 4, 5) fall approximately along the join $Na_4Ca_8Al_{20}Si_{20}O_{80}$-$Na_8Ca_4Al_{16}Si_{24}O_{80}$ (trend line III), and the composition range extends from close to that of end-member thomsonite, $\square_4Na_4Ca_8Al_{20}Si_{20}O_{80}\cdot 24H_2O$, to a composition close to $\square_4Na_6Ca_6Al_{18}Si_{22}O_{80}\cdot 24H_2O$. These compositions define the series $\square_4Na_{4+x}Ca_{8-x}Al_{20-x}$-$Si_{20+x}O_{80}\cdot 24H_2O$, where x varies from 0 to at least 2. The compositional variations of the gonnardite, tetranatrolite, and thomsonite crystalline series are summarized in Table 7.

The crystal structures of the minerals of the natrolite group

The crystal structure of natrolite was first proposed by Pauling (1930), and subsequently Taylor et al. (1933) determined the approximate location of all the atoms, ex-

TABLE 7. Crystalline series in the system Na_2O-CaO-Al_2O_3-SiO_2-H_2O*

1. Gonnardite series (measured values from $x \cong 0.3$–3.2)
   $\square_x Na_{16-3x}Ca_{2x}Al_{16+x}Si_{24-x}O_{80} \cdot nH_2O$
   (on the join $Na_{16}Al_{16}Si_{24}O_{80}$-$Na_4Ca_8Al_{20}Si_{20}O_{80}$)
2. Tetranatrolite series (measureed values from $x \cong 0.4$–3.9)
   $\square_0 Na_{16-x}Ca_xAl_{16+x}Si_{24-x}O_{80} \cdot 16H_2O$
   (on the join $Na_{16}Al_{16}Si_{24}O_{80}$-$Na_{12}Ca_4Al_{20}Si_{20}O_{80}$)
3. Thomsonite series (measured values from $x \cong 0$–2)
   $\square_4 Na_{4+x}Ca_{8-x}Al_{20-x}Si_{20+x}O_{80} \cdot 24H_2O$
   (on the join $Na_4Ca_8Al_{20}Si_{20}O_{80}$-$Na_8Ca_4Al_{16}Si_{24}O_{80}$)

* The symbol □ = vacant Na and Ca sites.

cept H, in the structure. Since that time a large number of crystal structure refinements of natrolite have been reported (Meier, 1960; Torrie et al., 1964; Peacor, 1973; Alberti and Vezzalini, 1981; Hesse, 1983; Pechar et al., 1983; Artioli et al., 1984; Kirfel et al., 1984; Baur et al., 1990), as well as of tetranatrolite (Mikheeva et al., 1986; Mazzi et al., 1986; Pechar, 1989), mesolite (Pechar, 1982; Artioli et al., 1986), scolecite (Fälth and Hansen, 1979; Joswig et al., 1984; Kvick et al., 1985), thomsonite (Alberti et al., 1981; Pluth et al., 1985; Ståhl et al., 1990), edingtonite (Galli, 1976), and tetraedingtonite (Mazzi et al., 1984). The crystal structure of gonnardite is unknown. Suffice to say, the crystal structures of the natrolite minerals thus far examined, with the exception of gonnardite, are generally well understood. However, except for one of the tetranatrolite structure determinations, all the structure determinations made thus far have been of crystals with end-member or close to end-member compositions. What are not understood are the structural mechanisms by which these minerals accommodate the variable amount of Na, Ca, and H_2O within the channels of the $[(Al,Si)_{40}O_{80}]$ framework to form the gonnardite, thomsonite, and tetranatrolite series. In the following, a review of the nature of the crystal structures of the natrolite minerals is presented with a view to obtaining a better understanding of the interrelationship between the structural elements and the chemical compositions.

The structure of the $[(Al,Si)_{40}O_{80}]$ framework

The crystal structures of the natrolite group minerals are based on a pseudo-tetragonal unit cell with $a \cong 13.1$ and $c \cong 6.6$ Å, the unit cell of tetranatrolite, the simplest of these structures. More complex crystallographic relations, caused by symmetry and dimensional adjustments required by compositional variations, are found in the other members of this mineral group (Table 2).

The basic structure of the natrolite minerals consists of $(Si,Al)O_4$ tetrahedra linked by corners to form chains oriented parallel to c; each chain is also linked to adjacent chains in one of three ways to form the three-dimensional framework. Slices of the natrolite framework taken parallel to the c-[110] and (001) planes are shown in Figures 6 and 7, respectively. The natrolite framework is characterized by the spiral linkage of adjacent tetrahedral chains, each chain being translated with respect to an

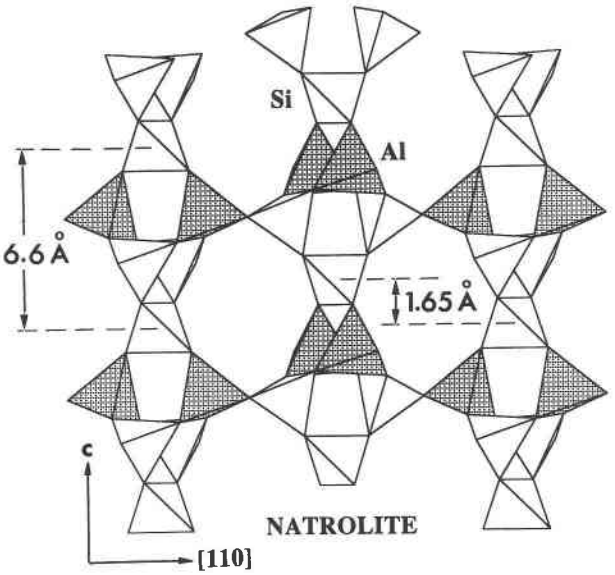

Fig. 6. Slice parallel to c-[110] of the natrolite framework. Si and Al tetrahedra share corners to form chains with a 6.6-Å repeat extending in the c direction; adjacent chains are linked in the [110] direction by sharing the bridging Si and Al tetrahedra. The adjacent chains are translated with respect to one another by $\pm 2c/8$ ($\cong 1.65$ Å). The intraframework Na and H_2O are not shown. This figure and Figures 7, 8, 12, 13, and 21 are based on the parameters given by Artioli et al. (1984).

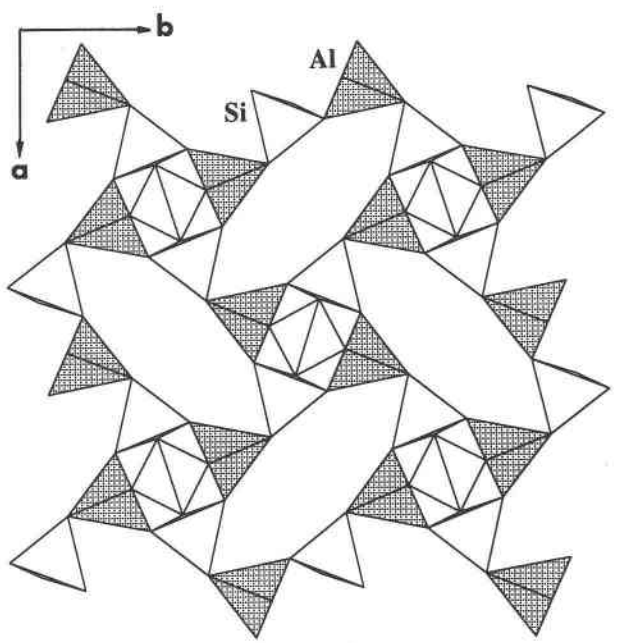

Fig. 7. Slice of the natrolite framework structure projected on (001). Four tetrahedral chains are linked together to form the large intraframework channels that contain Na and H_2O (not shown).

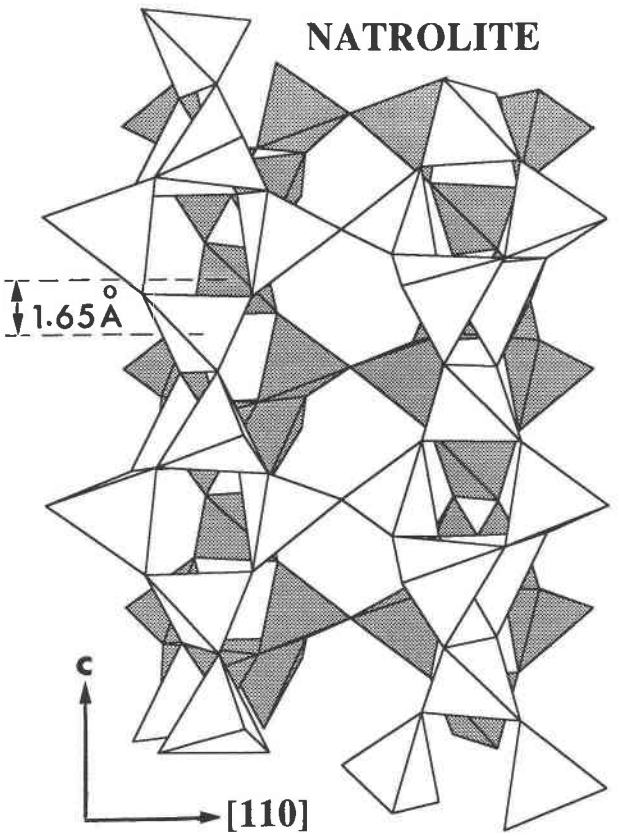

Fig. 8. Perspective drawing of the natrolite structure showing the natrolite-type linkage among four tetrahedral chains (front chains are white, rear chains are shaded). Each chain is translated with respect to an adjacent chain by approximately 1.65 Å ($\pm 2c/8$) such that the blocks of four adjacent chains form a spiral edifice.

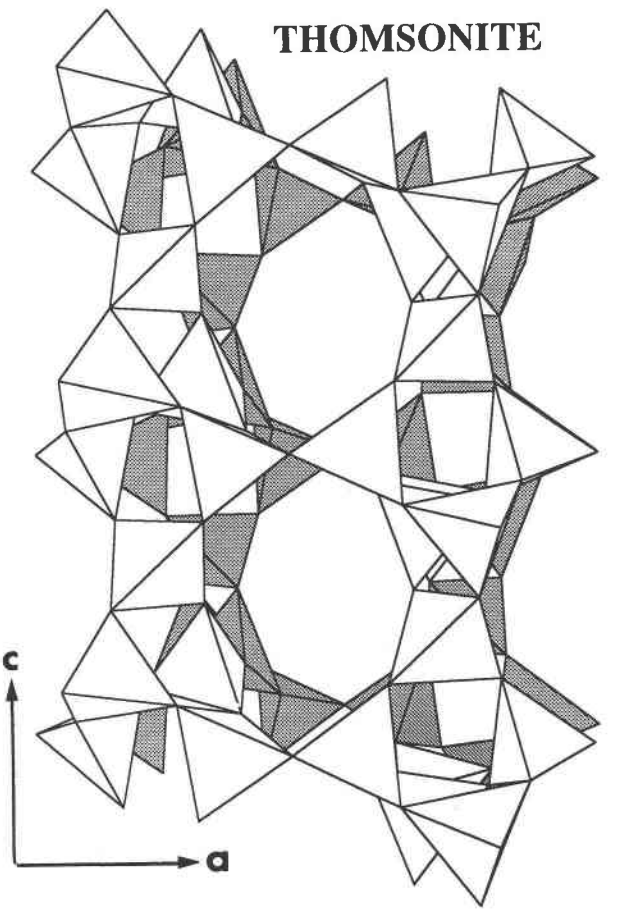

Fig. 10. Perspective drawing of the thomsonite structure showing the thomsonite-type linkage among four tetrahedral chains (chains in the front are white, those in the rear are shaded). The left pair of chains are translated parallel to c by approximately 1.65 Å relative to the right pair of chains.

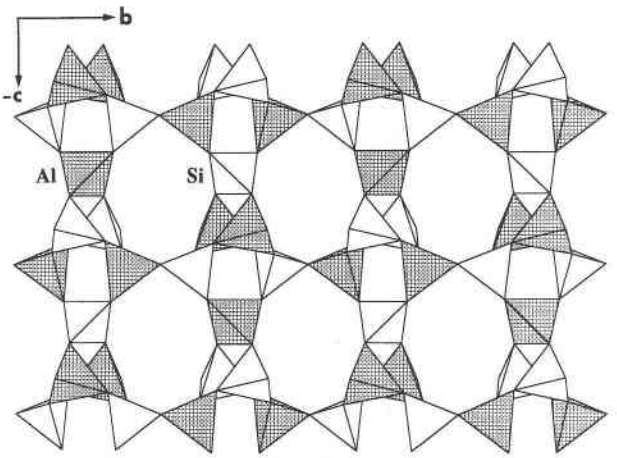

THOMSONITE

Fig. 9. Slice parallel to (100) of the thomsonite framework. The tetrahedral chains within this slice are linked together without any relative c-axis translations. This figure and Figures 10, 12, 14, 17, 18, and 21 are based on the parameters of Ståhl et al. (1990).

adjacent chain by $\pm 2\mathbf{c}$ (natrolite)/8 ($\cong$ 1.65 Å). The spiral linkage among four natrolite chains is shown in perspective in Figure 8. The framework of tetranatrolite, scolecite, and mesolite is also formed through the natrolite-type linkage of the chains and is topologically identical to that of natrolite. In the crystal structures thus far determined, Al and Si were found to be completely ordered in the scolecite and mesolite structures and in some, but not all, of the natrolite structures. Al and Si are partially to completely disordered in tetranatrolite.

A second way of linking the tetrahedral chains is found in the thomsonite structure. Within slices perpendicular to the **a** axis, the tetrahedral chains are not translated with respect to one another (Fig. 9), but within slices perpendicular to the **b** axis, adjacent chains are translated with respect to one another by $\pm \mathbf{c}$ (thomsonite)/8 ($\cong$ 1.65 Å), the same chain relationship as seen in the **c**-[110] slice of natrolite shown in Figure 6. Figure 10, a perspective drawing of the thomsonite structure, shows the thomsonite-type linkage of the tetrahedral chains. None of the

crystal structure studies of thomsonite reported any Si-Al disorder in the tetrahedral sites.

The third type of tetrahedral chain linkage, the edingtonite-type linkage, is found in the edingtonite and tetraedingtonite structures (Fig. 11). In these structures there is no relative **c**-axis translation of the tetrahedral chains. Al and Si are completely ordered in edingtonite and completely disordered in tetraedingtonite.

The arrangement of the cations and H_2O molecules

The Si-Al-O framework of the natrolite group minerals contains continuous channels oriented parallel to the **c** axis. The channels are composed of linked cages, spaced 6.6 Å apart, that contain the Na, Ca, and Ba cations and the H_2O molecules. The size and shape of these cages is related particularly to whether the linkage of the tetrahedral chains is of the natrolite, thomsonite, or edingtonite type. Crystal structures with linkage of the natrolite type have the smallest cages (Fig. 8), those with linkage of the thomsonite type have intermediate-sized cages (Fig. 10), and those with linkage of the edingtonite type have the largest cages (Fig. 11). The size of the cages within each framework is also affected by the amount of rotation of the tetrahedra (Gottardi and Galli, 1985, p. 37).

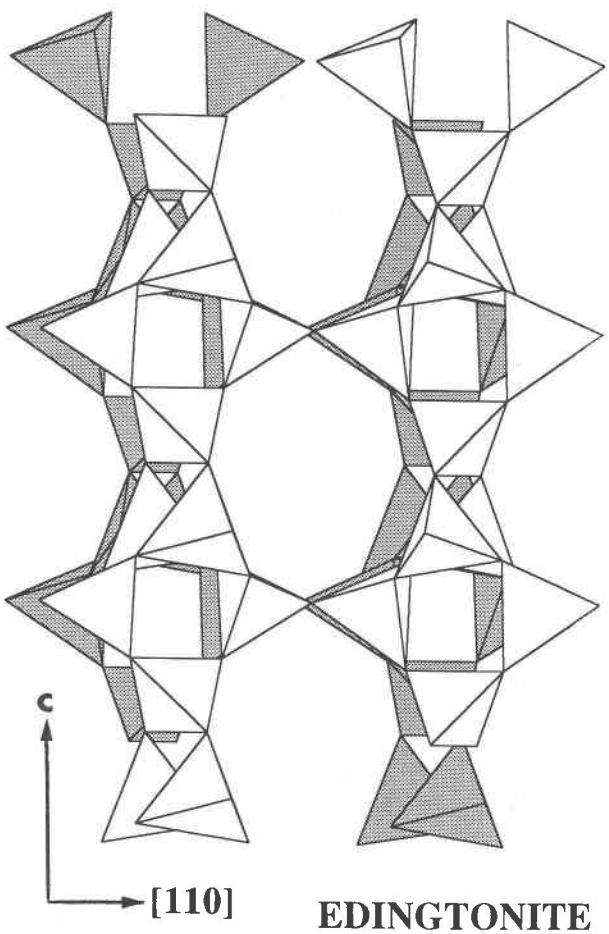

Fig. 11. Perspective drawing of the framework of the edingtonite crystal structure showing the edingtonite-type linkage among four tetrahedral chains (chains in front are white, those in the rear are shaded). There is no **c**-axis translation between the tetrahedral chains. This figure and Figures 14 and 21 are based on the parameters of Galli (1976).

Natrolite and tetranatrolite. Each channel cage in the natrolite structure contains two Na atoms, the Na atoms being coordinated by four O atoms from the framework and two H_2O molecules to form $NaO_4(H_2O)_2$ polyhedra. These polyhedra are in the shape of a distorted trigonal prism and link by sharing edges to form a continuous chain (Fig. 12). A perspective view of the complete natrolite structure looking down the channels is shown in Figure 13. The channels in the tetranatrolite structure contain polyhedra nearly identical in shape to those found in natrolite (Fig. 12). In tetranatrolite, however, up to 25% of the Na in the cages can be replaced by Ca, and a single cage can contain zero or one but not two Ca atoms.

Scolecite. The scolecite channels contain Ca atoms coordinated by four framework O atoms and three H_2O molecules to form a distorted pentagonal bipyramid. Each cage within the channels contains one Ca atom and one vacancy; thus the $CaO_4(H_2O)_3$ bipyramids do not link together as in natrolite but are isolated from one another (Fig. 14). To express the concept of vacancies within the crystal structure, the formula for scolecite can be written as $\square_8Ca_8Al_{16}Si_{24}O_{80}\cdot 24H_2O$.

Mesolite. The mesolite structure contains two types of channels. One type contains linked $NaO_4(H_2O)_2$ polyhedra that are nearly identical to those found in natrolite (Fig. 12); the second type contains isolated $CaO_4(H_2O)_3$ polyhedra nearly identical to those found in scolecite (Fig. 14). One-third of the mesolite channels contain Na poly-

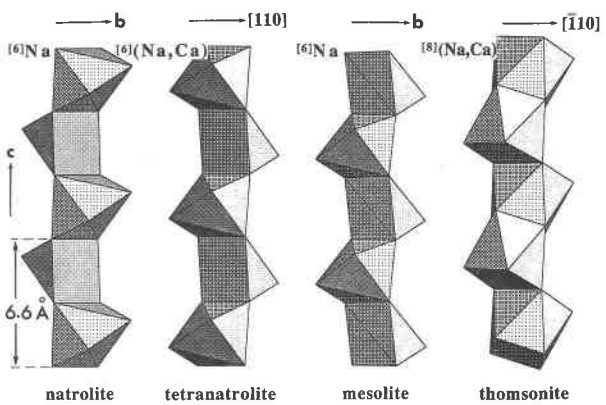

Fig. 12. Comparison of the Na-bearing coordination polyhedra of the natrolite minerals. In natrolite, tetranatrolite, and mesolite, the $NaO_4(H_2O)_2$ and $(Na,Ca)O_4(H_2O)_2$ polyhedra are nearly identical distorted trigonal prisms. The $(Na,Ca)O_4(H_2O)_4$ polyhedra about the hybrid Na,Ca site in thomsonite are in the form of regular square antiprisms. Number in brackets is the cation coordination number. Na,Ca refers to a disordered site in which Ca randomly replaces up to 50% of the Na. The tetranatrolite drawing is based on the parameters of Konnert and Ross (sample R18930, unpublished data).

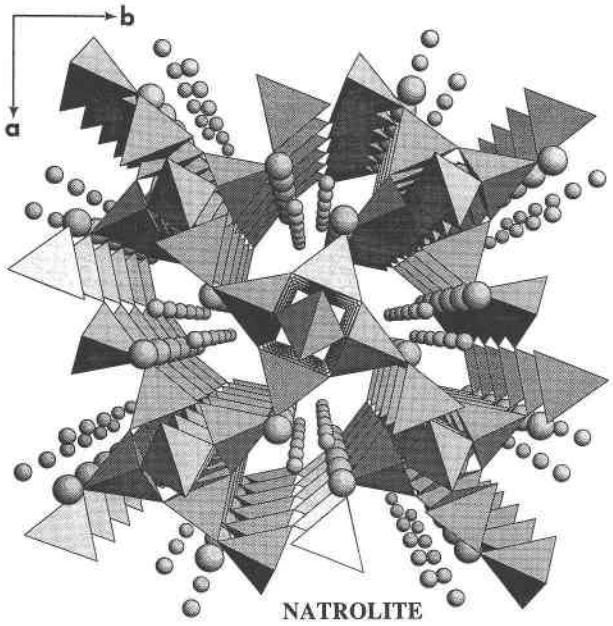

Fig. 13. A perspective drawing of the natrolite crystal structure viewed looking down the intraframework channels that contain Na atoms (smaller spheres) and H_2O molecules (larger spheres).

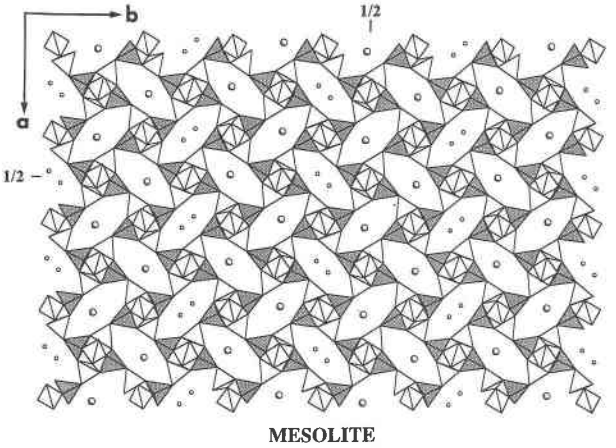

Fig. 15. A slice of the mesolite structure projected on (001). Al tetrahedra are shaded. The larger spheres are Ca atoms; the smaller spheres are Na atoms (H_2O not shown). This figure and Figures 12, 14, and 16 are based on the parameters of Artioli et al. (1986).

hedra and two-thirds contain Ca polyhedra, as seen in Figure 15, which shows a slice of the structure projected on (001). The mesolite structure may be thought of as composed of polysomes, each polysome consisting of one (010) slice of natrolite and two (010) slices of scolecite. In theory, a polysomatic series (Thompson, 1978) can be constructed of polysomes composed of *m* slices of scolecite with *n* slices of natrolite. The relative arrangement of the Na and Ca polyhedra within the channels is seen in Figure 16, which shows a slice of the mesolite structure

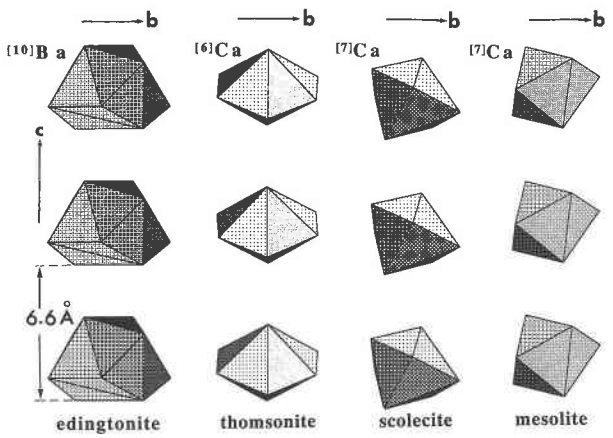

Fig. 14. Comparison of the coordination polyhedra occurring in edingtonite, $[BaO_6(H_2O)_4]$; thomsonite, $[CaO_4(H_2O)_2]$; scolecite, $[CaO_4(H_2O)_3]$; and mesolite, $[CaO_4(H_2O)_3]$. The scolecite drawing is based on the parameters of Fälth and Hansen (1979).

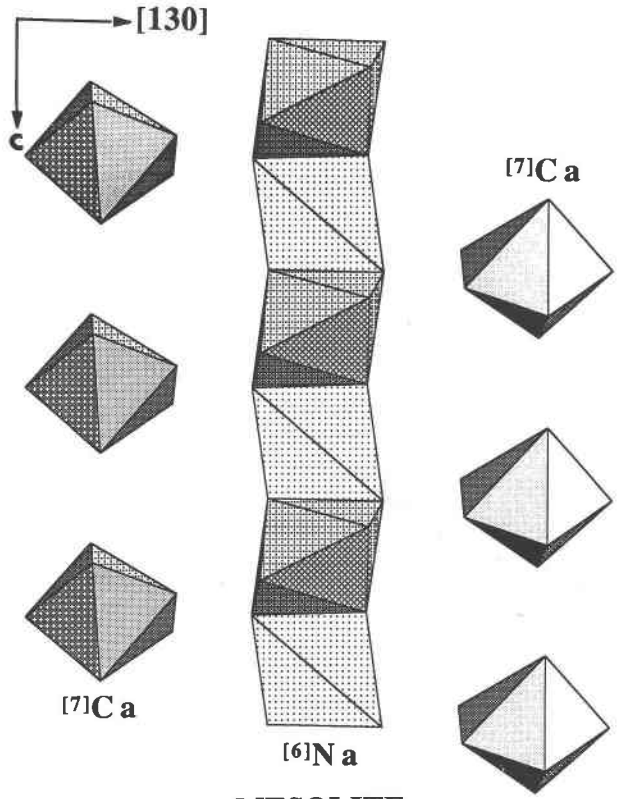

Fig. 16. A slice parallel to the c-[130] plane of the mesolite structure (excluding the Si-Al tetrahedra) showing the configuration of the $CaO_4(H_2O)_3$ and $NaO_4(H_2O)_2$ polyhedra. The Ca polyhedra are separated by vacant cation positions.

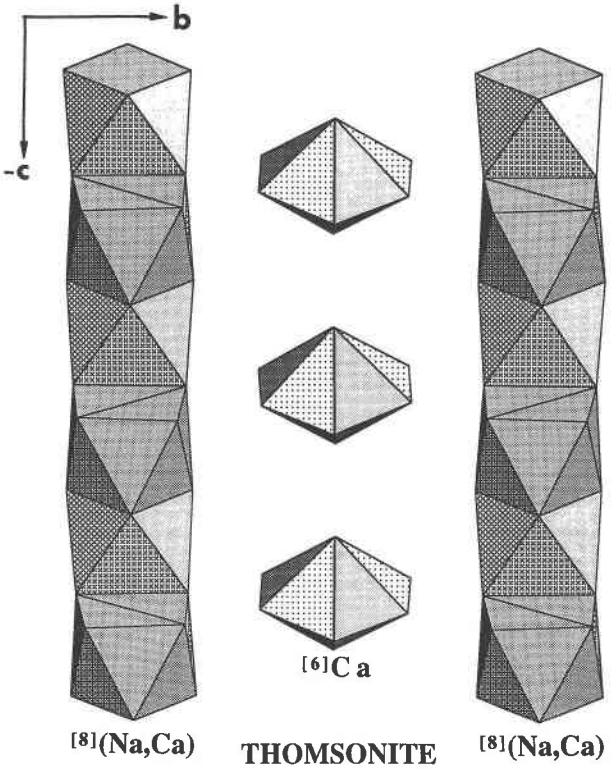

Fig. 17. A slice parallel to the **b**-**c** plane of the thomsonite structure (excluding the Si-Al tetrahedra) showing the configuration of the $(Na,Ca)O_4(H_2O)_4$ and $CaO_4(H_2O)_2$ polyhedra. The Ca polyhedra are separated by vacant cation positions.

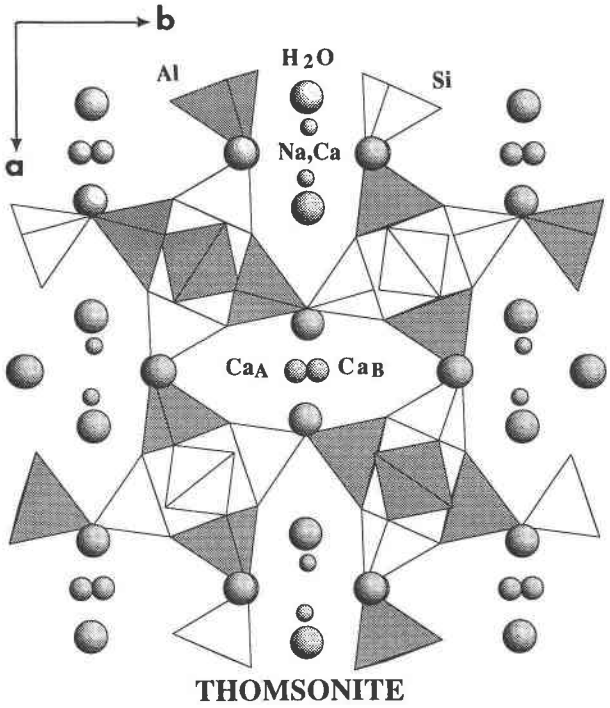

Fig. 18. A slice of the thomsonite structure projected on (001). The Al tetrahedra are shaded. The small, intermediate, and large spheres are Na, Ca, and H_2O, respectively. The Ca atoms occupy a split-atom position, and only one of the two positions pictured (Ca_A or Ca_B) is filled.

parallel to the **c**-[130] plane. The formula of the unit-cell contents of mesolite is $\square_{16}Na_{16}Ca_{16}Al_{48}Si_{72}O_{240}\cdot 64H_2O$, which expresses the 1/1 ratio of Na to vacancies and Na to Ca.

Thomsonite. The thomsonite framework also contains two types of channels. One type contains one Ca atom and one vacancy per cage, similar to that found in scolecite. The single Ca atom can occupy one of two positions, 0.52 Å apart, about a split-atom site. The isolated $CaO_4(H_2O)_2$ polyhedra are in the form of very distorted trigonal prisms. These Ca coordination polyhedra appear as hexagonal bipyramids in Figure 17, but, because Ca occupies only one of two possible positions about the center of this bipyramid, the pair of O atoms on the right side or on the left side of the bipyramid lie outside the Ca coordination sphere.

The second type of channel contains two atoms per cage. In end-member thomsonite, $\square_4Na_4Ca_8Al_{20}Si_{20}O_{80}\cdot 24H_2O$, there is one Na and one Ca atom in each cage, but these atoms are disordered within the channels. In the more sodic varieties of thomsonite, the channels contain approximately 70% Na and 30% Ca (Fig. 5, Table 4). The $(Na,Ca)O_4(H_2O)_4$ coordination polyhedra about the hybrid Na,Ca site are in the form of regular square antiprisms (Fig. 17). A slice of the thomsonite crystal structure projected on (001) is shown in Figure 18.

Edingtonite. In the edingtonite structure each channel cage contains a Ba atom and a vacancy. The Ba atom is coordinated by six O atoms and four H_2O molecules to form the complex polyhedra shown in Figure 14.

The Na-bearing polyhedra found in natrolite, tetranatrolite, mesolite, and thomsonite are compared in Figure 12. The Ba- and Ca-bearing polyhedra found in edingtonite, thomsonite, scolecite, and mesolite are compared in Figure 14.

The structural basis for the gonnardite, tetranatrolite, paranatrolite, and thomsonite crystalline series

A summary of the essential features of the nine natrolite mineral structures is presented in Figure 19; five of these minerals have structures with the natrolite-type framework, one with the thomsonite- and two with the edingtonite-type framework, and one possibly composed of more than one type of framework. To the right of each mineral name given in Figure 19 is recorded the cation content and cation coordination number within a single channel cage. As presented previously, natrolite, scolecite, and mesolite show only small deviations from the ideal formulas given in Table 1; thus there is no compelling evidence that these phases form a crystalline series with other members of the natrolite group. The compositions of edingtonite and tetraedingtonite also show little deviation from the ideal composition given in Table 1.

The tetranatrolite and paranatrolite series

The tetranatrolite series (series II, Table 7, Figs. 4, 5) involves the substitution of Ca for Na simultaneously with the replacement of Si by Al. No vacant sites appear in the channel cages (□ = 0). The principle of Al-Al avoidance in a framework of corner-sharing tetrahedra, plus review of the many reported chemical analyses, indicates that no more than 20 Al atoms can appear in the formula unit of any of the natrolite minerals (Table 1). Thus, in the tetranatrolite series, if maximum Al = 20, then the maximum Ca = 4. This maximum value of four atoms of Ca is approached in sample 86-53A, where Ca = 3.833 (Table 5, analysis 23). The Al-Si and Na-Ca substitutions and the presence of tetragonal space group *I*42*d* require at least partial Al-Si disorder in one or both tetrahedral sites and complete Na-Ca disorder within the channel cage sites. The three tetranatrolite structures thus far determined (Mazzi et al., 1986; Mikheeva et al., 1986; Pechar, 1989) show complete Na-Ca disorder and partial to nearly complete Al-Si disorder in both the T1 and the T2 sites. A recent structure refinement of tetranatrolite R18930 (J. A. Konnert and M. Ross, unpublished data) also shows complete Na-Ca disorder and nearly complete Al-Si disorder in the T1 and the T2 sites.

The cloudy crystals in samples R18930 and R16517 are composed mostly of tetranatrolite and twinned natrolite, respectively, and both phases appear to be decomposition products of paranatrolite. Since natrolite deviates little from the ideal composition $Na_{16}Al_{16}Si_{24}O_{80}\cdot 16H_2O$, dehydration of a Ca- and Al-rich paranatrolite (e.g., $Ca_4Na_{12}Al_{20}Si_{20}O_{80}\cdot 24H_2O$) to form natrolite requires a large change in the Al/Si ratio and thus a complete reorganization of the tetrahedral framework. Such a reaction should be very sluggish; the preferred reaction would be the formation of tetranatrolite, where minimal chemical and structural changes are required. A Ca- and Al-poor paranatrolite, possibly the precursor to the twinned natrolite in sample R16517, could much more readily form natrolite, since the transformation requires little change in the composition or crystal structure. Chao (1980) indicates that the symmetry of paranatrolite may be monoclinic. If this is so, then the origin of the twinning in the cloudy crystals of sample R16517 may be explained if monoclinic paranatrolite can transform into the orthorhombic noncentric natrolite in two orientations, that is, by forming right-handed and left-handed structures related to one another by a 90° rotation about a common **c** axis.

Our chemical studies show that the phase from Norway, reported as "gonnardite" by Mazzi et al. (1986), is actually tetranatrolite; the composition is $(Na,K)_{12.86}Ca_{3.00}Al_{18.44}Si_{21.46}O_{80}\cdot 24.8H_2O$ and is recorded in Figure 5 by the "x" mark. In the Fourier difference maps obtained during their crystal structure refinement, weak extra peaks appeared, which suggested that there were additional H_2O molecules in the channel cages. These peaks could perhaps be due to diffraction from residual domains of undehydrated paranatrolite within the tetranatrolite crystal.

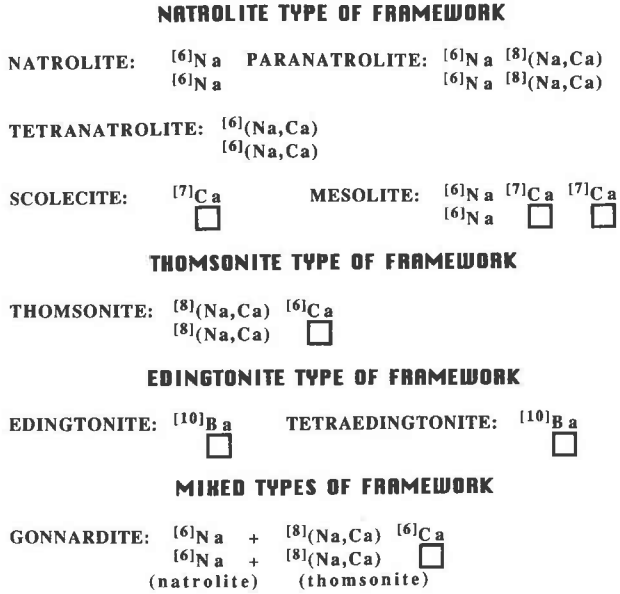

Fig. 19. Classification of the nine natrolite minerals according to the type of tetrahedral framework and composition of the channel cages within the framework. Each cage can contain two Na atoms, two atoms that include both Na and Ca, one atom of Ca plus a vacancy, or one atom of Ba plus a vacancy. The mesolite, thomsonite, and possibly the paranatrolite structures contain two types of cages. The gonnardite structure may be composed of mixed slabs of natrolite, $\square_0Na_{16}Al_{16}Si_{24}O_{80}\cdot 16H_2O$, and thomsonite, $\square_4Na_4Ca_8Al_{20}Si_{20}O_{80}\cdot 24H_2O$. Channel cation vacancy is indicated by □.

It is suggested that the tetranatrolite series, depicted in Figure 5 and defined in Table 7, also defines the paranatrolite series as $\square_0Na_{16-x}Ca_xAl_{16+x}Si_{24-x}O_{80}\cdot 24H_2O$, where $x \leq 4$. Paranatrolite has the natrolite-type framework, which is inherited by tetranatrolite or natrolite on dehydration. On the basis of the estimate of H_2O content in paranatrolite of 24 H_2O per formula unit (Chao, 1980) and the chemical composition of tetranatrolite presented here, it is postulated that the paranatrolite framework contains two types of channels. Each cage within the first type of channel contains two Na atoms coordinated by four O atoms and two H_2O. These $NaO_4(H_2O)_2$ polyhedra link to form chains similar to those found in natrolite (Fig. 12). Each cage within the second type of channel also contains two atoms (either Na-Na or Na-Ca), both coordinated by four O atoms and four H_2O molecules. These $(Na,Ca)O_4(H_2O)_4$ polyhedra link to form chains similar to those found in thomsonite (Fig. 17). In the second type of channel, Na and Ca are statistically distributed on the cation sites with a maximum of 50% Ca occupancy within the channel.

The thomsonite series

The thomsonite series (series III, Table 7, Figs. 4, 5) also involves the concomitant replacement of Ca with Na and Al with Si. In contrast to the tetranatrolite series,

where cage vacancies are zero, there are four vacant cage sites per formula unit, all of which are found in the channels that contain only Ca (in the tetranatrolite and thomsonite series the vacancies are fixed at 0 and 4, respectively). The composition limits of series III are defined by $16 \leq Al \leq 20$; note that the chemical analyses of the natrolite minerals rarely record less than 16 or greater than 20 Al atoms per formula unit. In the theoretical sodic end-member, $\square_4Na_8Ca_4Al_{16}Si_{24}O_{80} \cdot 24H_2O$, the hybrid Na,Ca site contains only Na. An X-ray structure determination of a thomsonite sample from Death Valley, California (Alberti et al., 1981), and neutron diffraction studies at 293 and 13 K of thomsonite from an unknown locality (Pluth et al., 1985; Ståhl et al., 1990) show no statistically significant Al-Si disorder in the six T sites but complete disorder of Na and Ca in the hybrid Na,Ca site. In all three determinations, the Ca site was found to be split into two positions, 0.3 Å apart, with approximately 10% of the Ca replaced by Sr. Even though the crystal structure of thomsonite has been determined by the most modern techniques, there is still some question as to whether the structure is fully defined. Pluth et al. (1985) observed 58 reflections that violated the extinction criteria for space group *Pncn*. In our examination of three thomsonite samples, we found that the sample from Drain, Oregon, showed violations of the two *n* glides, indicating that the space group for this sample is $Pmc2_1$, *P2cm,* or *Pmcm* rather than *Pncn* (Table 2).

The gonnardite series

The gonnardite series (series I, Table 7, Figs. 2, 3, 4) is the most complex of the three series in that the number of cation vacancies in the channel cages vary linearly with Ca content, approximately along the join $Na_{16}Al_{16}Si_{24}O_{80}$-$Na_4Ca_8Al_{20}Si_{20}O_{80}$. We present here a structural model to explain this series.

Diffraction data for gonnardite. Repeated and unsuccessful attempts were made to obtain good single-crystal X-ray photographs of gonnardite for symmetry and crystal structure analysis. The patterns were all poor because the crystal fragments examined were invariably multicrystalline. The distributions of the more intense reflections in the precession photographs of gonnardite from sample R10022 are very similar to that seen in the natrolite photographs. The X-ray powder patterns of the natrolite minerals are very similar, but the pattern of gonnardite shows distinct differences from those of natrolite, tetranatrolite, and thomsonite. With the hope that electron diffraction methods might be more informative, we asked Kenneth Livi (Department of Earth and Planetary Sciences, Johns Hopkins University) to examine sample R10022. Dispersed grain mounts were prepared from a fine fraction of the ground sample and examined with a Philips 420ST electron microscope equipped with instrumentation for analytical electron microscopy (AEM). Single crystals of gonnardite and thomsonite from sample R10022 were easily identified by AEM, which gave compositions very similar to those reported here (Tables 3, 4, Fig. 4) and proved that the analyses obtained with the electron microprobe were not from a mixture of phases. The single-crystal electron diffraction patterns of thomsonite were consistent with space group *Pncn* as reported in the literature (Table 2). The stronger subcell reflections in the single-crystal electron diffraction patterns of gonnardite are consistent with space group *Fdd*2 of natrolite (Table 2). However, extra rows of reflections appear in the **c***-[110]* and **a***-[031]* nets (Fig. 20), indicating a doubling of the repeat in the **a**, **b**, and **c** directions over those of the subcell. The subcell of gonnardite may be similar to that of natrolite, but the supercell is complex. Lattice-fringe imaging of the gonnardite crystals could not be accomplished because the finely focused electron beam

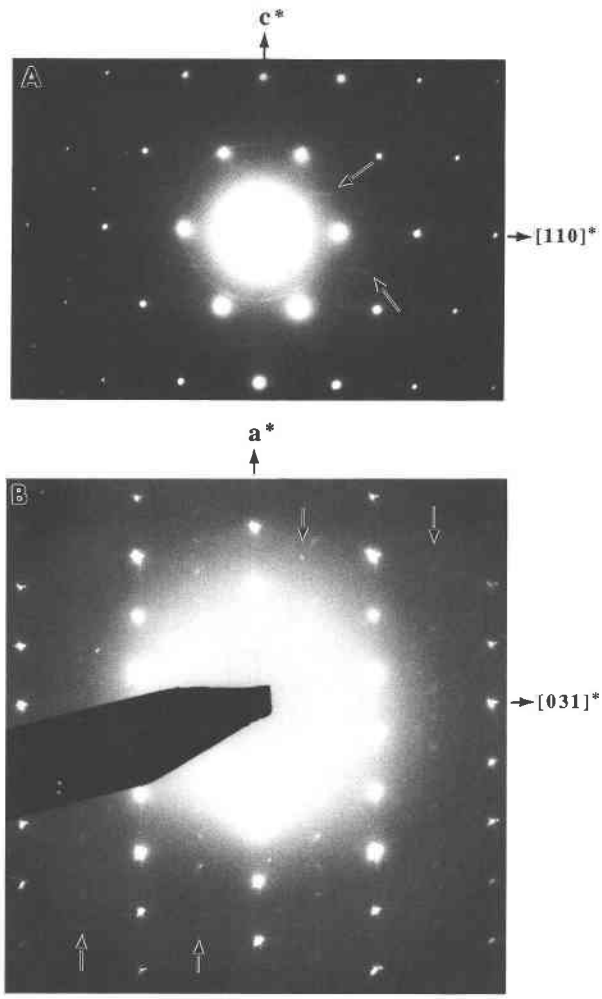

Fig. 20. Single-crystal electron diffraction patterns of gonnardite sample R10022. Patterns are indexed on a subcell corresponding to space group *Fdd*2 of natrolite (Table 2). (**A**) The **c***-[110]* net showing rows (arrows) of diffuse reflections having a nonorthogonal intensity distribution. These rows lie parallel to [110]* and between the rows of strong spots of the natrolite-like subcell. (**B**) The **a***-[031]* net showing extra rows (arrows) of reflections oriented parallel to **a*** and lying between the rows of strong reflections of the subcell.

caused decomposition. Electron diffraction and AEM, however, were undertaken without crystal decomposition.

A structural model for the gonnardite series. The compositional variation and complex unit cell of gonnardite can be explained if the gonnardite series is a polysomatic series composed of mixed domains of natrolite and thomsonite. There are two ways in which two different natrolite group framework structures can be joined on a coherent interface: (1) at an interface joining $(\bar{1}10)$ of natrolite with (010) of thomsonite, with the **c** axes parallel (Fig. 21A) and (2) at an interface joining $(1\bar{1}0)$ of edingtonite with (100) of thomsonite, with **c** axes parallel (Fig. 21B). Two polysomatic series can thus be constructed by interleaving slabs of natrolite and thomsonite or edingtonite and thomsonite. If gonnardite is indeed composed of interleaved slices of natrolite and thomsonite, the extensive chemical variation of gonnardite samples reported in Figures 2, 3, and 4 and the complex crystallographic relations of sample R10022 can be understood. A series composed of mixing m slabs of end-member natrolite, $\square_0Na_{16}Al_{16}Si_{24}O_{80}\cdot 16H_2O$, with n slabs of end-member thomsonite, $\square_4Na_4Ca_8Al_{20}Si_{20}O_{80}\cdot 24H_2O$, fairly well describes the gonnardite compositions given in Figures 2, 3, and 4, although there is considerable scatter in gonnardite H-45-8 (Fig. 2), perhaps due to the presence of a second phase. However, the gonnardite phases in the three samples from Puy de Dome, France (157727, 15273, and 138378), have compositions that deviate significantly from trend line I (Fig. 4). The compositions of gonnardite and thomsonite in sample 157727 (Fig. 1E) are plotted in Figure 22. The gonnardite data points fall approximately on trend line IV. Trend IV defines a polysomatic series composed of slices of end-member natrolite and slices of sodic thomsonite of composition $\square_4Na_{5.5}Ca_{6.5}Al_{18.5}Si_{21.5}O_{80}\cdot nH_2O$. Proof of the existence of such mixed structures must await lattice-fringe imaging by TEM using cold stages and very low energy electron beams. Lastly, there is the question of whether gonnardite has a true stability field or rather is metastable with respect to natrolite + thomsonite or natrolite + mesolite. The textures of coexisting gonnardite and thomsonite in the Magnet Cove samples (Figs. 1A, 1B) suggest, however, that these two minerals are in equilibrium.

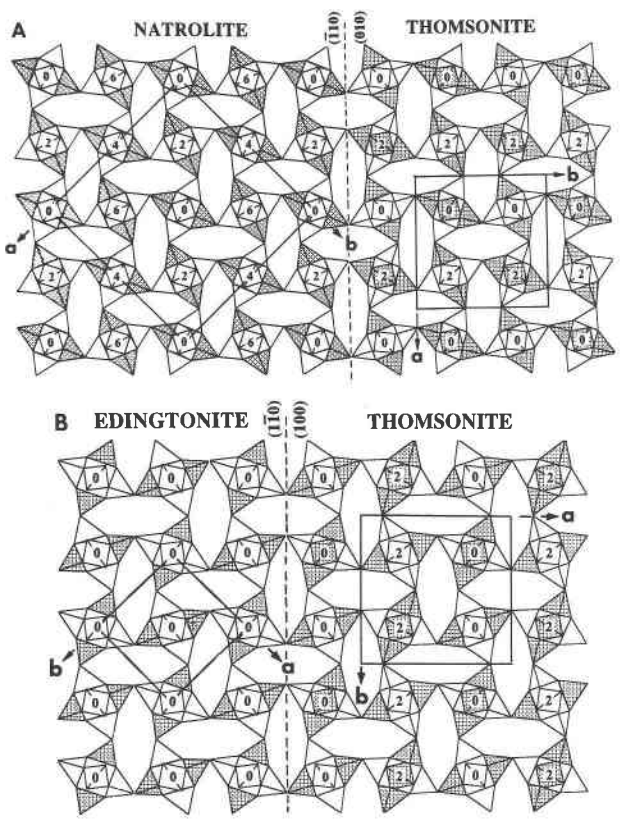

Fig. 21. The two possible ways of joining two different tetrahedral frameworks on a coherent interface. Al-bearing tetrahedra are shaded. The numbers 0, 2, 4, and 6 give the height of the central tetrahedra above the (001) plane in multiples of c(natrolite)/8 (Alberti and Gottardi, 1975; Gottardi and Galli, 1985, p. 37). (**A**) Projection of the natrolite and thomsonite structures on (001). The two lattices are joined at a coherent interface (dashed line), which is parallel to $(\bar{1}10)$ and (010) of natrolite and thomsonite, respectively. (**B**) Projection of the edingtonite and thomsonite structures on (001). The coherent interface (dashed line) is parallel to the $(1\bar{1}0)$ and (100) planes of edingtonite and thomsonite, respectively.

Discussion

Although a great deal is now known about the composition and structure of the natrolite minerals, little is

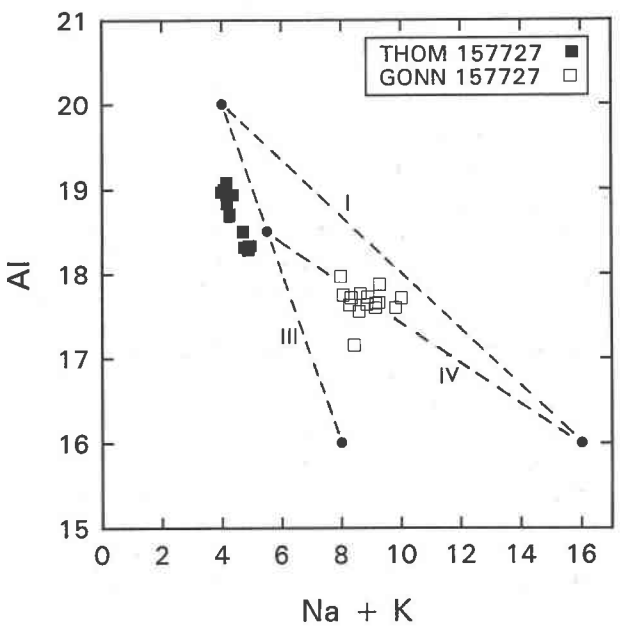

Fig. 22. Compositional trends for coexisting gonnardite and thomsonite in sample 157727 from Puy de Dome, France (Fig. 1E). Trends I and III and small closed circles are as in Figure 5. Trend IV lies on the join $Na_{16}Al_{16}Si_{24}O_{80}$-$\square_4Na_{5.5}Ca_{6.5}Al_{18.5}Si_{21.5}O_{80}$, also denoted by small closed circles.

known of their stability fields (Gottardi, 1989). Experimental studies of zeolite equilibria are greatly hampered by slow reaction rates and difficulties in nucleation. Senderov and Khitarov (1971) reported that natrolite-type and analcime-type zeolites formed under stable conditions from amorphous materials in the temperature range of 100–200 °C. We are not aware of any other reports of equilibrium synthesis of any of the nine natrolite minerals. Quantitative estimates of the conditions of natural formation of these minerals are also scarce; however, Kristmannsdóttir and Tómasson (1978) reported that thomsonite, mesolite, and scolecite formed in the Icelandic geothermal areas in the temperature range of 65–100 °C. Carpenter (1971) presents a theoretical activity-activity diagram indicating stability fields at low P and T for natrolite, mesolite, and thomsonite and compares this diagram with naturally occurring thomsonite- and mesolite-bearing assemblages observed in the altered basalts at Cape Blomidon, Nova Scotia.

The natrolite minerals occurring in the Magnet Cove syenites are formed as a result of late-stage reaction of the primary nepheline, the latter having reequilibrated or, possibly, crystallized at temperatures as low as 500 °C (Flohr and Ross, 1989). The metasomatic alteration may be the result of autometasomatism, or deuteric alteration, in which early magmatic phases react with their own residual fluids to form a suite of low-temperature minerals such as natrolite, gonnardite, and thomsonite. In the case of the alteration of nepheline occurring in the mafic ijolite xenoliths, the metasomatism may have occurred when the xenoliths were entrained in the volatile-rich magma of the host garnet pseudoleucite syenite. The jacupirangite may have experienced low temperature metasomatism that was related to the formation of nearby mineral deposits or was metasomatized by circulating late-stage hydrothermal fluids during the waning stages of igneous activity at Magnet Cove. Autometasomatism cannot be ruled out. The literature cited above would suggest that the Magnet Cove zeolites formed below 200 °C.

The many reports on natural occurrences of the natrolite group minerals and the need to understand the conditions under which these minerals crystallized indicate that renewed efforts should be made in determining their stability fields. Our present study suggests a number of problems that may be encountered in equilibrium experiments besides those of kinetics and nucleation; for example, the presence of at least three crystalline series, the presence of possibly metastable phases and the dehydration products of paranatrolite, the difficult of phase identification by conventional X-ray powder methods, the role of Al-Si and Na-Ca order-disorder in obtaining equilibrium, and choosing geologically pertinent experimental variables.

Acknowledgments

We thank Jeffrey Post (U.S. National Museum, Washington, DC) for helping us with sample acquisition and for his much appreciated advice on our X-ray powder diffraction work and crystal drawings, James McGee (U.S. Geological Survey, Reston) for his help with various aspects in the use of the electron microprobe, Harvey Belkin (U.S. Geological Survey, Reston) for his help in sample preparation, Judith Konnert (U.S. Geological Survey, Reston) for her crystal structure analysis of the Mont Saint-Hilaire tetranatrolite, and Kenneth Livi (Johns Hopkins University) for analyzing one of our thomsonite-gonnardite specimens with the transmission electron microscope and furnishing us with several electron diffraction patterns and chemical analyses. Lastly, we wish to acknowledge that our present understanding of the structure of the natrolite minerals is, in no small way, due to the studies of the late Professor Glauco Gottardi and his colleagues at the University of Modena—we dedicate this paper to the memory of this distinguished mineralogist.

References cited

Alberti, A., and Gottardi, G. (1975) Possible structures in fibrous zeolites. Neues Jahrbuch für Mineralogie Monatshefte, 9, 396–411.

Alberti, A., and Vezzalini, G. (1981) A partially disordered natrolite: Relationships between cell parameters and Si-Al distribution. Acta Crystallographica, B37, 781–788.

Alberti, A., Vezzalini, G., and Tazzoli, V. (1981) Thomsonite: A detailed refinement with cross checking by crystal energy calculations. Zeolites, 1, 91–97.

Alberti, A., Pongiluppi, D., and Vezzalini, G. (1982) The crystal chemistry of natrolite, mesolite and scolecite. Neues Jahrbuch für Mineralogie Abhandlungen, 143, 231–248.

Artioli, G., Smith, J.V., and Kvick, Å. (1984) Neutron diffraction study of natrolite, $Na_2Al_2Si_3O_{10}\cdot 2H_2O$, at 20 K. Acta Crystallographica, C40, 1658–1662.

Artioli, G., Smith, J.V., and Pluth, J.J. (1986) X-ray structure refinement of mesolite. Acta Crystallographica, C42, 937–942.

Baur, W.H., Kassner, D., Kim, C.-H., and Sieber, N.H. (1990) Flexibility and distortion of the framework of natrolite: Crystal structures of ion-exchanged natrolites. European Journal of Mineralogy, 2, 761–769.

Birch, B. (1989) Chemistry of Victorian zeolites. In W.D. Birch, Ed., Zeolites of Victoria, special publication 2, p. 91–102. The Mineralogical Society of Victoria, Melbourne, Australia.

Carpenter, A.B. (1971) Graphical analysis of zeolite mineral assemblages from the Bay of Fundy area, Nova Scotia. In American Chemical Society Advances in Chemistry Series, 101, 328–333.

Chao, G.Y. (1980) Paranatrolite, a new zeolite from Mount St-Hilaire, Québec. Canadian Mineralogist, 18, 85–88.

Chen, T.T., and Chao, G.Y. (1980) Tetranatrolite from Mount St-Hilaire, Québec. Canadian Mineralogist, 18, 77–84.

Deer, W.A., Howie, R.A., and Zussman, J. (1963) Rock-forming silicates, vol. 4: Framework silicates. Longman, London.

Dowty, E. (1991) Atoms (Macintosh version 1.0). Shape Software, Kingsport, Tennessee.

Fälth, L., and Hansen, S. (1979) Structure of scolecite from Poona, India. Acta Crystallographica, B35, 1877–1880.

Flohr, M.J.K., and Ross, M. (1989) Alkaline igneous rocks of Magnet Cove, Arkansas: Metasomatized ijolite xenoliths from Diamond Jo quarry. American Mineralogist, 74, 113–131.

——— (1990) Alkaline igneous rocks of Magnet Cove, Arkansas: Mineralogy and geochemistry of syenites. Lithos, 26, 67–98.

Foster, M.D. (1965a) Compositional relations among thomsonites, gonnardites, and natrolites. U.S. Geological Survey Professional Paper 504-E, E1–E10.

——— (1965b) Composition of zeolites of the natrolite group. U.S. Geological Survey Professional Paper 504-D, D1–D7.

Galli, E. (1976) Crystal structure refinement of edingtonite. Acta Crystallographica, B32, 1623–1627.

Gottardi, G. (1989) The genesis of zeolites. European Journal of Mineralogy, 1, 479–487.

Gottardi, G., and Galli, E. (1985) Natural zeolites. Springer-Verlag, Berlin.

Gunter, M.E., Knowles, C.R., and Schalck, D.K. (1991) Intergrown natrolite/mesolite "single" crystals from the Columbia River basalts. Geological Society of America Abstracts with Programs, 23, A219.

Hesse, K.-F. (1983) Refinement of a partially disordered natrolite, $Na_2Al_2Si_3O_{10}\cdot 2H_2O$. Zeitschrift für Kristallographie, 163, 69–74.

Hey, M.H. (1933) Studies on the zeolites. Part V. Mesolite. Mineralogical Magazine, 23, 421–447.

——— (1936) Studies on the zeolites. Part IX. Scolecite and metascolecite. Mineralogical Magazine, 24, 227–253.

Joswig, W., Bartl, H., and Fuess, H. (1984) Structure refinement of scolecite by neutron diffraction. Zeitschrift für Kristallographie, 166, 219–223.

Kile, D.E., and Modreski, P.J. (1988) Zeolites and related minerals from the Table Mountain lava flows. Mineralogical Record, 19, 153–184.

Kirfel, A., Orthen, M., and Will, G. (1984) Natrolite: Refinement of the crystal structure of two samples from Marienberg (Usti nad Labem, CSSR). Zeolites, 4, 140–146.

Kristmannsdóttir, H., and Tómasson, J. (1978) Zeolite zones in geothermal areas in Iceland. In L.B. Sand and F.A. Mumpton, Eds., Natural zeolites, occurrence, properties, and use, p. 277–284. Pergamon, New York.

Krogh Anderson, E., Danø, M., and Peterson, O.V. (1969) A tetragonal natrolite. Meddelelser om Grønland, 181, 1–19.

Kvick, Å., Ståhl, K., and Smith, J.V. (1985) A neutron diffraction study of the bonding of zeolitic water in scolecite at 20 K. Zeitschrift für Mineralogie, 171, 141–154.

Mazzi, F., Galli, E., and Gottardi, G. (1984) Crystal structure refinement of two tetragonal edingtonites. Neues Jahrbuch für Mineralogie Monatshefte, 8, 373–382.

Mazzi, F., Larsen, A.O., Gottardi, G., and Galli, E. (1986) Gonnardite has the tetrahedral framework of natrolite: Experimental proof with a sample from Norway. Neues Jahrbuch für Mineralogie Monatshefte, 5, 219–228.

Meier, W.M. (1960) The crystal structure of natrolite. Zeitschrift für Kristallographie, 118, 430–444.

Mikheeva, M.G., Pushcharovskii, D.Yu., Khomyakov, A.P., and Yamnova, N.A. (1986) Crystal structure of tetranatrolite. Soviet Physics and Crystallography, 31, 254–257.

Nawaz, R. (1988) Gonnardite and disordered natrolite-group minerals: Their distinction and relations with mesolite, natrolite and thomsonite. Mineralogical Magazine, 52, 207–219.

Nawaz, R., Malone, J.F., and Din, V.K. (1985) Pseudomesolite is mesolite. Mineralogical Magazine, 49, 103–105.

Pabst, A. (1971) Natrolite from the Green River Formation, Colorado, showing an intergrowth akin to twinning. American Mineralogist, 56, 560–569.

Pauling, L. (1930) The structure of some sodium and calcium aluminosilicates. Proceedings of the National Academy of Sciences U.S.A., 16, 453–459.

Peacor, D.R. (1973) High-temperature, single crystal X-ray study of natrolite. American Mineralogist, 58, 676–680.

Pechar, F. (1982) Precise definition of the crystalline structure of natural mesolite. Acta Montana, 59, 143–152.

——— (1989) An X-ray determination of the crystal structure of natural tetragonal natrolite. Zeitschrift für Kristallographie, 189, 191–194.

Pechar, F., Schäfer, W., and Will, G. (1983) A neutron diffraction refinement of the crystal structure of natural natrolite, $Na_2Al_2Si_3O_{10}\cdot 2H_2O$. Zeitschrift für Kristallographie, 164, 19–24.

Pluth, J.J., Smith, J.V., and Kvick, Å. (1985) Neutron diffraction study of the zeolite thomsonite. Zeolites, 5, 74–80.

Rychly, R., and Ulrych, J. (1980) Mesolite from Horni Jilove, Bohemia. Tschermaks mineralogische und petrographische Mitteilungen, 27, 201–208.

Senderov, E.E., and Khitarov, N.I. (1971) Synthesis of thermodynamically stable zeolites in the Na_2O-Al_2O_3-SiO_2-H_2O system. In American Chemical Society Advances in Chemistry Series, 101, 149–154.

Ståhl, K., Kvick, Å., and Smith, J.V. (1990) Thomsonite, a neutron diffraction study at 13 K. Acta Crystallographica, C46, 1370–1373.

Taylor, W.H., Meek, C.A., and Jackson, W.W. (1933) The structures of the fibrous zeolites. Zeitschrift für Kristallographie, 84, 373–398.

Thompson, J.B., Jr. (1978) Biopyriboles and polysomatic series. American Mineralogist, 63, 239–249.

Torrie, B.H., Brown, I.D., and Petch, H.E. (1964) Neutron diffraction determination of the hydrogen positions in natrolite. Canadian Journal of Physics, 42, 229–240.

Ulrych, J., and Rychly, R. (1983) Re-examination of the natrolite group zeolites from the Ceske Stredohori Mts., NW Bohemia, Czechoslovakia. Acta Universitatis Carolinae—Geologica, Rost Volume, (1–2), 33–52.

Manuscript received March 4, 1992
Manuscript accepted March 20, 1992